GEOLOGICAL SURVEY OF CANADA
OPEN FILE 6868

Assessing permafrost conditions and landscape hazards in support of climate change adaptation in Pangnirtung, Nunavut

A.-M. LeBlanc, M. Allard, A.-S. Carbonneau,
G.A. Oldenborger, E. L'Hérault, W.E. Sladen, P. Gosselin, and D. Mate

2011

Natural Resources Canada
Ressources naturelles Canada

Canada

GEOLOGICAL SURVEY OF CANADA
OPEN FILE 6868

Assessing permafrost conditions and landscape hazards in support of climate change adaptation in Pangnirtung, Nunavut

A.-M. LeBlanc, M. Allard, A.-S. Carbonneau, G. A. Oldenborger, E. L'Hérault, W.E. Sladen, P. Gosselin, and D. Mate

2011

doi:10.0495/289548

This publication is available from the Geological Survey of Canada Bookstore (http://gsc.nrcan.gc.ca/bookstore_e.php).
It can also be downloaded free of charge from GeoPub (http://geopub.nrcan.gc.ca/).

Recommended citation:
LeBlanc, A.-M., Allard, M., Carbonneau, A.-S., Oldenborger, G.A., L'Hérault, E., Sladen, W.E., Gosselin, P., and Mate, D., 2011. Assessing permafrost conditions and landscape hazards in support of climate change adaptation in Pangnirtung, Nunavut. Geological Survey of Canada, Open File 6868, 65 p. doi:10.4095/289548

Publications in this series have not been edited; they are released as submitted by the author.

CONTENTS

LIST OF FIGURES

EXECUTIVE SUMMARY

Climate change can have an impact on urban development and infrastructure in the Arctic as permafrost temperature and active layer thickness increase and, also, as more frequent extreme climatic events trigger landscape hazards. The Canada-Nunavut Geoscience Office (CNGO) launched the "Nunavut Landscape Hazard Mapping Initiative" in 2009 to provide geoscience information and expertise to Nunavut communities in order to support them in developing adaptation and management strategies that incorporate anticipated climate changes. Under this initiative, a study of permafrost conditions was undertaken in the Hamlet of Pangnirtung by the Geological Survey of Canada (GSC) and Université Laval's Centre d'études nordiques (CEN). Pangnirtung was seriously affected by an extreme rain event in June 2008, which has led to severe permafrost degradation along the Duval River banks due to thermal erosion.

On a community scale, ground investigations remain the most effective way of characterizing permafrost conditions. A combination of mapping, shallow and deep drilling, sampling, shallow geophysical surveys, ground thermal instrumentation, and snow surveys was used during the summer 2009 and winter 2010 field seasons. This Open File outlines the methodology used in the field and presents current permafrost conditions based on the results of the 2009/10 investigation, including the surficial geology, ground ice content and ground thermal regime of Pangnirtung. These results form the baseline information needed to assess the landscape hazards and permafrost sensitivity to climate warming or any human disturbances and, therefore, support community planning. Results are not only targeted to the community of Pangnirtung, but also to engineers and land use planners working in the North, since the methodology and results can be transferable to other northern communities and Arctic environments.

Prior to the field work, airphoto interpretation was conducted to identify the surficial geology and delineate landscape features associated with permafrost. The airphoto interpretation was reassessed in the field. During summer 2009, pits were dug to the thaw front and the underlying permafrost was cored with a portable earth drill. The samples were kept frozen for laboratory analysis (ice and water contents, salinity, grain size, Atterberg limits, and radiocarbon dating). In addition, two deep (~15 m) holes were drilled with an airtrack drill. Thermistor cables were installed in the deep boreholes and in two additional shallow (~3 m) boreholes to monitor the permafrost temperatures in different terrain units. These cables supplement a cable that was installed by the GSC the previous year. Miniature loggers equipped with a single temperature sensor were buried in the near surface (~5 cm) at various sites across the village to monitor the soil surface temperatures and, therefore, provide information on the surface thawing and freezing indices. Two types of shallow geophysical surveys were conducted in the study area: ground penetrating radar and electrical resistivity using both a capacitively-coupled resistivity meter and a multi-electrode galvanic resistivity meter. These data are more extensive, spatially continuous, and provide deeper subsurface information than the mapping and drilling data. Finally, in March 2010, the snow cover was characterized in order to correlate snow properties and soil surface temperatures.

Four main areas of Pangnirtung, distinguished by their unique terrain features, were first identified by airphoto interpretation and thereafter investigated in the field (see Figure 12): 1) the alluvial fan through which the Duval River flows, 2) the alluvial terrace with boulders and eroded channels along the banks of the Duval River, 3) the till terrace covered by colluvium to the east of the alluvial fan, also known to be the next development area of the community, and 4) the marine sediments covered by colluvium to the west of the alluvial fan. Results are shown on: 1) the distribution of ice-rich permafrost and its relationship to the surficial geology, 2) the thickness of the surficial and underlying layers and, 3) the different ground thermal regime in each distinctive terrain type. An ice-rich colluvium blanket was found throughout the studied areas, but mostly in the sectors to the west and east of the town. On the east side of the Duval River, in addition to the ice-rich colluvium, a network of ice wedges may exist in the underlying till. The thickness of the colluvium blanket is estimated to be between 1 and 3 m and is probably discontinuous over the area. The thickness of the marine sediments appears quite variable, but generally appears to increase from west to east, especially on the south side of the runway. The thickness of the alluvial fan varies from about 2 to 10 m with the greater thickness appearing to be on the south-west portion of the alluvial fan. The alluvial fan overlies a till deposit as seen in the eroded bluff face, except close to the coastline near the mouth of the Duval River where sandy, silty and shell-rich marine sediments were found underlying the alluvial fan deposit. The thickness of the till to the east of the alluvial fan is at least 15 m, since bedrock was not encountered during drilling.

Permafrost was warmer in the vicinity of the alluvial fan and colder away from it to the east and west. At 12 m depth, the ground temperatures are -2.8, -5.2, and -7.1 ºC in the alluvial fan, in the marine sediments at the airport, and in the till terrace to the east, respectively. In the marine sediments, the maximum thaw depth in 2009 varied from 0.75 m to 1.8 m (measured at three locations), while in the till terrace and the alluvial fan it was about 1 and 2.5 m, respectively. Surface thawing indices varied from 725 (natural conditions) to 1263 (gravel road) degree days, while freezing indices ranged from 756 (thick snow cover) to 3029 (bare road) degree days.

Such difference in sediment types, ice content and permafrost temperatures will eventually lead to a spatially variable thermal and physical response of the permafrost to climate warming. The area along the river currently represents the most vulnerable geological sector in the community. The permafrost is warmer there than in any other area in the community, especially where snow drifts accumulate along the river bank. Coarse grained material, typical of the alluvial fan, exhibits a greater thermal response to changes in air temperature than fine-grained material, and therefore, the ground thermal regime of this area is expected to respond more rapidly to climate warming. The physical response (i.e. ground subsidence) has also proved to be high close to the river due mainly to the underlying till, which consists of a fine-grained matrix easily eroded during high discharge of the Duval River. Although the other areas studied have colder permafrost, the presence of ice-rich permafrost within the colluvium cover could eventually lead to thaw settlement if the active layer thickness increases. Possible ice wedges in the till terrace add to the sensitivity of this area to climate warming or human disturbances. Some care must be taken not to channel surface water flow into frost cracks in order to prevent thermal erosion and gullying. A complete assessment of the landscape hazards related to permafrost degradation and a more detailed study of the thermo-erosion

processes along the Duval River are underway. These will provide further tools in support of the economic development through infrastructure maintenance and community planning in Pangnirtung.

1 INTRODUCTION

Permafrost underlies northern communities and, under an equilibrium thermal state, provides a stable foundation for infrastructure. However, over the past decades, the Canadian Arctic has experienced significant increases in air temperature and the scientific community agrees that climate change is expected to continue (ACIA 2005, IPCC 2007). Several observations indicate that permafrost conditions have already started to change in response to the recent warming (Smith et al., 2010, Smith et al. 2005, Allard et al. 2002). For instance, in Iqaluit, permafrost temperatures at a depth of 5 m have increased by about 2 °C per decade since the early '90s (Throop 2010). To maintain the integrity of existing infrastructure and to ensure that new infrastructure is designed appropriately, it is essential to acquire good knowledge of surficial geology and permafrost conditions.

A study of permafrost conditions was undertaken in the Hamlet of Pangnirtung, Nunavut, by the Geological Survey of Canada (GSC) and Université Laval's Centre d'études nordiques (CEN), under the Landscape Hazard Mapping Program run by the Canada-Nunavut Geosciences Office (CNGO). Some urgency justified the start of the program in Pangnirtung as it was seriously impacted in June 2008 by an extreme peak discharge of the Duval River, which flows through the center of the community. In a matter of several hours, the river cut a section about 240 m long and nearly 10 m deep in a reach near the coast, eroding its bed and its banks and damaging the town's main bridge, thus cutting off a large part of the hamlet from its water supply. In addition, as outlined in the recent Pangnirtung community plan and zoning by-law report, the hamlet's growing population needs new housing and urban expansion is required. Therefore, many development constraints were identified, including the steep slope adjacent to the existing built-up area and the limited tracts of flat land (FoTenn and Trow 2007). However, no consideration was given to soil types, permafrost conditions, or permafrost sensitivity. The extreme rain event that occurred in 2008 and the permafrost degradation that followed provide a relevant example that geoscientific data need to be incorporated into community planning.

The aims of this project are: 1) to provide high quality baseline information on permafrost conditions in the main soil types found in the community, 2) to assess landscape hazards related to possible permafrost destabilization caused by climate warming and human disturbances and, 3) to provide better knowledge of permafrost sensitivity in the area to support decision-making processes in community planning and improve strategies for community development.

This Open File is a summary of the methodology used in the field and provides results of surficial geology and current permafrost conditions, including its thermal state, after one year of measurements. Field methods include mapping of surficial geology, shallow and deep drilling, geophysical surveying, recording of air, ground and surface temperatures, and snow measurements.

Ground temperature recording instrumentation was put in place in boreholes, initiating a monitoring program aimed at measuring the impacts of climate change on permafrost, namely active layer variations and the evolution of the permafrost thermal regime over the coming years. Based on these initial results, a brief discussion is presented on the permafrost sensitivity in the area. Because this report is targeted to stakeholders, land use planners and engineers, the terrain type map is shown as the main result. The interpretation of geophysical surveys and shallow boreholes observations are integrated into the description of the terrain units. This extends the information obtained through the airphoto interpretation and field observations both spatially and vertically. Not all the surficial deposits found in Pangnirtung are described in detail in this report; the focus is instead on the main terrain units subject to development (FoTenn and Trow 2007) or related to recent permafrost degradation. Surface and ground temperatures are discussed in separate sections, while snow measurements are incorporated into the interpretation of the thermal regimes. However, ground temperatures are also discussed in relation to terrain types.

2 SITE DESCRIPTION

2.1 GENERAL

Pangnirtung is an Inuit community of about 1300 people located on Baffin Island just below the Arctic Circle, at 66º5' N latitude and 65º45' W longitude (Figure 1). The village is located on the southern shore of Pangnirtung Fjord, which opens onto Cumberland Sound. Established on coastal terraces at the foot of high rocky cliffs, the community has limited space for expansion. The airport occupies an important tract of land enclosed within the urbanized area. Current expansion is gradually taking place eastwards from the Duval River (FoTenn and Trow 2007). This area is of limited extent and constitutes the last available flat space where construction is relatively easy.

2.2 GEOLOGY

The surficial geology consists of till in the form of Late Pleistocene lateral moraines, the Duval Moraines, found along the base of the mountain (Dyke 1977), and as a thick deposits making up the terraces downslope of the moraines (Smith et al. 1989). North of the airport, the hamlet occupies a promontory which is underlain by post-glacial marine sediments consisting of sand overlying clayey silts (Aitken and Gilbert 1989). The maximum elevation of the post-glacial marine submergence was reported to be about 50 m above present sea level (Dyke 1979, Aitken and Gilbert 1989). However no geomorphic or sedimentary indicator such as a clearly visible raised beach could be identified within the community area, and our surveys seem to indicate that the marine limit is at about 40 m. Bedrock outcrops along the shoreline of this promontory and is metamorphic gneiss of Precambrian age (Isherwood and Smith 1983, Smith et al. 1989). The central part of the study area lies on a coarse alluvial fan at the mouth of the Duval River. The alluvial fan was first mapped as a raised delta (Isherwood and Smith 1983, Smith et al. 1989) and more recently as an alluvial terrace (Dyke, in press).

2.3 CLIMATE

The mean annual air temperature (MAAT) and annual precipitation for the period 1925 to 1950 were -8 ºC and 336 mm, respectively (Dyke 1977). During the period from 1950 to the early 1990s, the high eastern Arctic was characterized by a cooling climate (Throop et al. 2010). Maxwell (1980) and Hyatt et al. (2003) reported mean annual air temperatures of -10 ºC and -8.9 ºC, respectively, but the time periods of observation were not provided. Masterton and Findlay (1976) reported an average of 395 mm of precipitation annually, of which 44% occurs as rain between June and September.

Recent data from Environment Canada (Environment Canada 2009) for the period 1996 to 2009 indicate a warmer climate, with a MAAT of -7.6 ºC and an increase in rain precipitation. Between 1996 and 2007, Pangnirtung received nearly 200 mm of precipitation during summer months, which is about 54% of the annual precipitation. The MAAT at Pangnirtung is warmer than the more southern community of Iqaluit where the MAAT for the same period (1996-2009) is -8.4 ºC.

2.4 PERMAFROST

Pangnirtung lies within the continuous permafrost zone (Hegginbottom et al. 1995). Permafrost temperatures at depths of 15 m, recorded from thermistor cables installed in till near the current water reservoir between 1988 and 1991, ranged from -6.5 to -7.5 ºC (Hyatt 1998). Ground temperatures in a number of areas throughout the community ranged from -3 to -8 ºC at depths of 8 m (Isherwood and Smith 1983, Smith et al. 1989), but precise locations of these measurements are not always known. More recently, permafrost temperatures, ranging from -2.9 to -4.1 ºC at depths of 15 m, were measured manually in five boreholes located near the Duval River bridge (Hsieh and Tchekhovski 2008 - not for release). In most areas, the maximum active layer thickness varies from 0.5 to 1.5 m, except in coarser deposits where thaws depths can reach up to 3 m (Smith et al. 1989).

None of the thermistor cables installed in previous studies are currently functioning. Therefore, until recently, no ground temperature data were available to reflect the climate warming of the last decade. With funding from the Federal Government's International Polar Year (IPY) Program, the GSC established a Nunavut permafrost monitoring network (Ednie and Smith 2010). In 2008, a thermistor cable was installed, at the airport near the Environment Canada weather station, in collaboration with the Pangnirtung hamlet. The mean annual ground temperature (MAGT) at this site is -5.2 ºC at 15 m depth. Ground temperature data from this cable are integrated into the present study.

2.5 ADDITIONAL BACKGROUND INFORMATION

Several relevant studies in addition to those mentioned above are mentioned briefly here. Hyatt et al. (2003) report on the presence of buried glacier ice in the highest moraines above the hamlet. Hyatt (1992) also observed tunnelling in the moraines above the hamlet due to flowing creek water. An excellent description of observations of permafrost in sandy till and of an ice-wedge network acquired during the excavation of the municipal water reservoir is found in Hyatt (1990) and Smith et al. (1989). Smith and Dallimore (1980, 1981) report on the surficial geology, geotechnical properties

of soils, and depth to bedrock around Pangnirtung. Beneath the intertidal flats, the bedrock surface was found to drop off steeply from the shore where the flats are narrow, whereas near the mouth of the Duval River where the flats are wide, it is nearly level and covered by approximately 30 m of sediment (Pullan et al. 1983).

3 METHODS USED AND FIELD WORK

To characterize the permafrost conditions and integrate all the geoscientific information into a high resolution map for the Pangnirtung area, a variety of mapping and field methods were used. Each subsection below describes the purpose and usefulness of the methods and, if necessary, the concept behind the method. The field work was done in August 2009, March 2010, and May and June 2010. Details of the field investigations and the location of the surveys and instrumentation are also provided in the subsections below and are shown in Figure 2.

3.1 AIR PHOTOGRAPH INTERPRETATION AND MAPPING

Airphoto interpretation is a fast and economical method used to delineate the surficial geology and landscape features such as thermokarst, gelifluction landforms, and ice wedge polygons. This process is effective in planning a field investigation (Allard et al. 1991), as identification of these features reveals information about the local ground and climatic conditions that can later be verified in the field.

Black and white air photographs from 1976 at a scale of 1:6000 were used to delineate the major surficial deposits and landscape features and make a preliminary surficial geology map of the area. The interpretation was reassessed in the field using stratigraphic sections, core samples, and geophysics. A natural stratigraphic section in the bank of the Duval River was described and sampled to provide information in the center of the study area where drilling was difficult because of the large number of boulders in the sediments. Other field observations are discussed below.

3.2 SHALLOW AND DEEP BOREHOLES

Undisturbed, 10 cm diameter cores were retrieved from shallow boreholes to characterise the surficial geology, to determine permafrost ice contents and structure, and to validate the mapping. This was done using a lightweight earth drill, specially designed for coring in frozen ground (Figure 3) (Calmels at al. 2005). This modified earth auger uses a STIHL 08 S engine mounted with a high rotation speed transmission and a diamond-impregnated carbide bit. The cores were kept frozen and sent to Laval University for laboratory testing to determine the geotechnical properties including: ice and water content, grain size distribution, salinity, and Atterberg Limits.

Due to depth limitations of the earth drill, an airtrack drill was used to obtain information on the geology at depth and to install ground temperature monitoring cables. While this method is fast and not restricted by rock, sampling is limited to cuttings circulated to the surface, making it difficult to

determine the depth from which they come (Figure 4). A total of 20 shallow (1-3.2 m) boreholes (SDH-01 to SDH-20) and two deep (13.9 and 14.9 m) boreholes (DDH-01 and DDH-02) were drilled.

3.3 GROUND TEMPERATURES

Because results from previous studies (e.g. Ednie and Smith 2010, Hsieh and Tchekhovski 2008, Hyatt 1998, Isherwood and Smith 1983, Smith et al. 1989) showed a high spatial variability in ground temperature within the municipal boundary of Pangnirtung, the field work included the installation of thermistor cables at sites representative of major geological units and in various topographic contexts. Continuous measurements of ground temperatures will not only ensure the recording of the current thermal conditions of the ground, but will also allow trends to be detected, and therefore, will allow a better understanding of the response of permafrost to climate change in coming years.

Thermistor cables consist of temperature sensors spaced at specific intervals which span the length of the cable. The cables were constructed in the field based on the site conditions and the maximum depth of the borehole. Thermistors utilised are YSI 44033, which have an accuracy of ±0.1°C. Two sixteen-channel and one eight-channel data loggers, manufactured by RBR Ltd., were attached to the cables to record measurements at one hour intervals. The boreholes were cased with 1¼" diameter PVC tubing and backfilled with the drill cuttings. The thermistor cables were placed within the PVC tubing which was then filled with silicone oil to avoid any heat by convection within the casing. For protection from the elements and vandalism, the data loggers were placed in 4" PVC tubes (Figure 5). A total of four thermistor cables were installed: two cables to depths of 2.7 and 3 m in SDH-14 and SDH-06, respectively, and two cables to depths of 13.9 and 14.9 m in DDH-01 and in DDH-02, respectively. These cables complement the 15 m-deep thermistor cable, DDH-Airport, installed by the GSC at the airport in 2008 (Ednie and Smith 2010).

3.4 AIR AND GROUND SURFACE TEMPERATURES

The thermal regime of permafrost is closely related to not only climate variability but also the surface conditions controlling the heat exchange between the ground and the air. To establish the thermal boundary conditions for a variety of ground surface conditions specific to Pangnirtung, miniature temperature loggers were used to measure ground surface temperature at specific locations at the same time as air temperature. This allows the determination of the freezing and thawing indices (sum of the degree day below or above zero, respectively), for both for the surface and air, and thus permits the calculation of n-factors (ratio of the surface index to the air index), which are widely used by engineers for thermal design of buildings and roads. With the knowledge of the subsurface conditions and the air temperatures, the ground surface temperatures can be used to infer the ground temperatures in deeper layers. An additional advantage to the miniloggers is that they are less expensive and easier to install than thermistor cables.

The miniature temperature loggers used are the HOBO Pro v2, manufactured by Onset (Figure 6). These waterproof miniloggers operate over a wide temperature range (-40 to 50 ºC) and have an accuracy of ±0.2°C. Data are recorded at one hour intervals in order to provide a continuous record

of ground surface temperatures. A total of nine HOBOs, labelled st-1 to st-9 (Figure 7), were buried in the near surface; four are adjacent to the thermistor cables and the remaining five were placed at sites with different ground surface conditions, such as a road, a wetland, a snow bank, etc. In addition, one HOBO was placed in a Stevenson shelter at the airport to record air temperature.

3.5 SNOW MEASUREMENTS

Among the parameters affecting surface conditions, snow cover is probably the most important because it is recognized as a good thermal insulator, preventing ground cooling in winter (Goodrich 1982). The spatial distribution of snow at a local scale depends on the snowfall, prevailing winds, vegetation, topography, obstacles and snow removal practices. To characterise the variability in snow cover around Pangnirtung and, therefore, infer qualitative information about the ground thermal conditions, measurements of snow density and thickness were made in March 2010. The Snow-Fork by Toikka Oy was used to measure snow density (Figure 8). The sensor is a steel fork which acts as a microwave resonator to measure electrical parameters from which the dielectric constant of snow and, therefore, the density of snow is calculated. Snow depth and density profiles were measured at each borehole and ground surface temperature site. In addition, measurements were made along two transects to capture snow thickness variability, one along the east side of the Duval River and the other along the road parallel to the fjord on the east side of the water reservoir.

3.6 GEOPHYSICS

Geophysical data provide information on the physical properties of the ground and on the spatial distribution of these properties. They are more extensive, spatially continuous, and provide deeper subsurface information than the mapping and drilling data. However, these data provide only proxy measurements of geology and permafrost conditions, and are thus subject to interpretation and should be considered as complimentary to other forms of ground truthing. In this study, ground penetrating radar (GPR) and electrical resistivity methods were used. The advantage of these two methods is that the physical properties measured are highly sensitive to the transition from unfrozen to frozen state.

3.6.1 GROUND PENETRATING RADAR (GPR)

Ground penetrating radar (GPR) is a non-destructive geophysical technique that involves the transmission of short radio waves (electromagnetic – EM - waves), from 10 to 1000 MHz, to map subsurface structures. The velocity of these EM waves are controlled by the dielectric constant of the ground, which is in turn dependant on material types, density and porosity, and water content. One antenna transmits a short pulse of EM energy to the subsurface; when an interface is reached such as a contrast in dielectric constant, the signal is then reflected back to the surface and detected by the receiving antenna. For instance, the dielectric constant of air is 1, 3 to 4 for ice, around 6 for frozen sediments, around 25 for unfrozen sediments, and 80 for fresh water (Moorman et al. 2003). The other electrical property involved is the electrical conductivity of the material, which influences the attenuation of the EM pulse. In highly conductive materials such as saturated clay, the depth of the penetration of the EM signal is low since the attenuation is high. The result of a GPR survey

appears as a collection of parallel traces, each trace being the two-way travel time of the EM pulse between the transmitter and the receiver. Knowing the travel time and the velocity of the EM wave, depth to reflectors are determined.

GPR surveys were carried out with a pulseEkko 1000 system from Sensors and Software Inc. (Figure 9) using antennas of 50, 100 and 200 MHz. Higher frequencies are attenuated more easily than low frequencies and therefore the depth of penetration is lower. However, higher frequencies provide better resolution than low frequencies. Therefore, the use of the three sets of antennas provides good coverage for the resolution and the depth of penetration needed. The antennas were mounted in a cart to facilitate the surveys. The data were recorded at equally spaced steps, with the interval depending on the antenna frequency, and were viewed in real-time on a screen attached to the cart. Initial GPR surveys were targeted to areas of importance for hazard identification (Duval River) and community planning (east side of town). In order to provide complete geographic coverage and additional information near the boreholes, additional data were collected along many segments over roads, beside Parks Canada's warehouse, and in the center of a natural area in the west part of town. Common Mid Point surveys (CMP) were also performed in different areas to obtain the velocity of the radar signal into the ground, and thus convert the travel time scale into a depth scale. For each survey profile, an average velocity was then used at all depths. Before the profiles were interpreted, filters to remove as much background noise as possible, gains to amplify the data at greater depths, and topographic corrections were applied.

3.6.2 ELECTRICAL RESISTIVITY

Electrical Resistivity Imaging (ERI) is a geophysical method that involves injection of a controlled electrical current into the ground, along with measurement of the electrical potential and its perturbation by geophysical targets or anomalies. The primary physical parameter governing the distribution of the electrical potential field is electrical conductivity, the reciprocal of electrical resistivity. Electrical conductivity is the most variable physical property of solid earth materials, easily spanning more than 10 orders of magnitude for rocks and sediments. In most geologic environments, electrical current is considered to propagate via electrolytic, or ionic, conduction through pore fluids. The electrical resistivity of permafrost depends on pore water salinity, pore size and shape, water content and degree of saturation, amount of clay and its mineral composition, and temperature and water phase. In permafrost materials, resistivity increases (or conductivity decreases) exponentially until most of the pore water is frozen (Pearson et al. 1983). In marine sediments, the higher conductivity of the pore water makes their resistivity exceptionally low.

Electrical resistivity imaging was carried out using a capacitively-coupled resistivity meter (CCR - Geometrics OhmMapper – Figure 10) and complementary data were collected at select sites using a multi-electrode galvanic resistivity meter (GR - IRIS Syscal R1+ Switch 48 – Figure 11). A Wenner survey geometry was used to m aximize signal strength in the pe rmafrost environment. Surveys were again targeted based on identification of hazards, community planning priorities, as well as areas near boreholes. The CCR system is composed of a coaxial cable with one transmitter and five receivers pulled by either a person or an ATV. This system is "non-contacting" in that it allows for acquisition of data where physical contact with the ground via electrodes is prohibitive, such as along

hamlet roads or where contact resistance with the ground is prohibitively high such as for ice or very dry soils. GR surveys involve injection of current directly into the ground via galvanic contact with a pair of current electrodes. The potential distribution is then measured across many pairs of voltage electrodes. Details of data acquisition, processing and inversion of electrical surveys performed in Pangnirtung are provided in Oldenborger (2010).

4 SURFACE GEOLOGY MAP

Although very well documented at the regional scale (Dyke, in press), the Quaternary geology remains imprecise at the community scale. An interpreted airphoto of Pangnirtung was published by Smith et al. (1989), however, that map was an exploratory one for a construction project and is not precise. More detailed information associated with this map was provided in several consultant reports (e.g. Smith and Dallimore 1980, Smith and Dallimore 1981, Isherwood and Smith 1983), but they are not easily available to the public and stakeholders. Therefore, a new community scale map of the surficial geology was prepared as part of this project (Figure 12).

The map shows that Pangnirtung is located on different terrain units, each underlain by a dominant surficial geological unit. The central sector of the map is occupied by a large Holocene alluvial fan of the Duval River; the soil consists of gravel, sand and boulders. In the distal part of the fan, towards lower elevations and the coastline, the sandy material contains marine shell fragments, indicating that the fan was deposited in contact with the sea. The fan was later incised by the Duval River, forming terraces along its trajectory.

The terrace to the east (where municipal expansion is taking place) is made of till covered by colluvium in the lower part. The colluvium consists of thin sand and gravel layers laid down by thin flows of water over the frozen surface during spring melt. This process has buried organic soil layers and up to 2 m of ice rich, new permafrost has accumulated on top of the pre-existing till deposits. The unit is characterized by areas of parallel drainage gullies and water tracks from which eroded sediments are transported, as well as other areas of poor drainage. Up-slope of that sector, the colluvial blanket vanishes where a lateral moraine (the youngest of the Duval moraines) extends along the foot of the steep valley side.

The airport is built mainly on marine sediments dating from the post-glacial sea transgression; the soils are dominantly composed of sand overlying silt. The origin of the sand cover is interpreted as colluvial. However, beach deposits could also be present between the colluvium and the silt (Aitken and Gilbert, 1989). The southern limit of this unit is not clearly defined due to the presence of a layer of colluvium, but appears to be close to 40 m elevation, agreeing well with the ≈50 m marine limit reported by others (Dyke 1979, Aitken and Gilbert 1989). Finally a layer of colluvium also covers the till at the foot of the valley wall south of the airport.

5 EXTENDED INFORMATION THROUGH CORING AND GEOPHYSICS

5.1 ALLUVIAL FAN OF THE DUVAL RIVER AND ALLUVIAL TERRACE WITH BOULDERS AND ERODED CHANNELS ALONG THE BANKS OF THE RIVER

5.1.1 STRATIGRAPHIC SECTION AND CORING

A good description of the alluvial fan and the alluvial terrace was obtained from a section along the river bank showing a 3 m thick layer of boulders, sand and gravel (Figure 13). However, the thickness of this layer seems to vary spatially based on the geophysical results (see below). This coarser upper layer agrees with two shallow boreholes which were terminated at 1 and 1.4 m depth due to boulders. The alluvial fan is underlain by fine to coarse grained sand with traces of silt and gravel (Figure 13). The lower unit is probably till, based on the poor sorting of the sediments, traces of angular coarse sand and gravel, and the absence of shells. Marine shells were observed in borehole SDH-18 and in a natural section close to the coastline on the east side of the Duval River mouth; they were also reported by Aitken and Gilbert (1989) on the west side of the Duval and by Hsieh and Tchekhovski (2008) at the lower reaches of the north side of the fan. The shells indicate that sea level was higher than at present when the fan was deposited. Therefore, in the southern, higher part of the fan, it appears to be underlain by till, while to the north of the bridge, the fan is underlain by marine sediments. In some parts of the boulder layer, the soil is a sequence of coarse oxidized sand with fine silt and some organics (Figure 14), interpreted as old alluvial channels. Several stratigraphic sections along the river banks contain alternating layers of sand-size alluvium and organic matter that represent past stages of overbank flow. Six of the organic layers were sampled and radiocarbon dated in an attempt to obtain an idea of when these high river stages occurred (Figure B1, stratigraphic section, Appendix B).

The active layer thickness in mid-August was 0.72 m at sites SDH-19 and SDH-01 and 1.4 m at site SDH-18, but can reach 2 to 3 m in some other areas based on the geophysical and thermal results. No ice lenses were found below the active layer, but the investigations were limited to the near surface.

5.1.2 GROUND PENETRATING RADAR

Borehole and stratigraphic section observations were used to interpret the GPR results. The GPR profile along the east side of the Duval River using the 200 MHz antennas is shown in Figure 15. Several boulders were identified in the upper layer by their hyperbolic signature. Old alluvial channels were also identified within the alluvial fan. The presence of the boulders tends to create interference, however, with the more or less parallel reflectors, usually interpreted as the thaw front, and the stratigraphic contact between the alluvial sediments and the underlying till. Therefore, a measurement of the thawing front at the SDH-19 site (0.72 m) at the time of the survey was used to guide delineation of the thaw front from the GPR data. However, thicker active layers were found away from the area of old channels, close to the Duval River (see Section 6), or in areas of standing water (see Section 5.1.3). Based on this GPR profile, the thickness of the alluvial sediments varies

from 2 to 4 m, but may be thicker at places where the contact line is dashed. Observations made by Smith and Dallimore (1981) indicate a gravelly and bouldery sand layer of about 4 to 7 m in the area of the survey line.

Based on the other GPR profiles (see Appendix A), the thickness of the alluvial fan is more than 10 m near the campground, the health center and south of the fire hall at the apex of the fan, but is less than 10 m along the road from the bridge to the airport. The marked lateral transition between the alluvial deposits and the marine sediments appears at about 300 m from the start of Line A4. From 0 to 300 m, the EM signal is rapidly lost due to the presence of marine silts and sands near the surface and below the road embankment. The same transition is well observed on Line A1 along the road to the campground. From the start until about 265 m along the GPR line, near the arena, the EM signal is rapidly lost due to the presence of marine sediments. At 265 m, the EM signal penetrates deeper in the alluvial deposits and reaches a depth of about 10 m before vanishing due to limit of penetration depth. At the ground surface, this lateral transition occurs at an elevation of ≈ 38 m. On survey Line A3, two lateral transitions appear that are consistent with the change from till to marine sediments, (again at about 38 m elevation) and from marine sediments to alluvial fan. Again, the presence of several boulders prevents the delineation of continuous reflectors. However, one strong continuous reflector does appear at a depth of 2 to 3 m in most of the survey lines below the road surface, and is interpreted as the thawing front.

5.1.3 ELECTRICAL RESISTIVITY

Capacitive and galvanic data were collected along the same Duval River section (Figure 16a) and capacitive data were collected along the arena-campground road (Figure 16b). Other capacitive and galvanic resistivity models in the alluvial area are presented by Oldenborger (2010). Comparing the different data types for the Duval River section, we see that the capacitive model yields lower resistivity values than the galvanic model. The GR survey results are generally less noisy, exhibit a better fit to the raw data, and are more accurately represented by the modelling algorithm. Hence, the GR results may be considered more "trustworthy" in terms of material property values. However, despite higher noise levels, the CCR data are collected at a much higher spatial sample interval and with smaller dipole separations such that the near-surface resolution is superior. It follows that the CCR models likely provide better estimates of depth and spatial extent for model features, particularly in the near surface.

The low resistivity (conductive) layer at the surface of the Duval River section corresponds to zones of standing water on the surface and is likely the signature of the active layer (~500 Ωm CCR ~1000 Ωm GR). Its thickness is variable across the section, reaching 2-3m depth in places towards the fjord and decreasing towards SDH-19. The middle layer of extremely high resistivity is interpreted to be very dry and porous gravel (as would be expected in alluvial deposits), very ice-rich or both (>30 kΩm CCR, >60 kΩm GR). A thick alluvial sheet is consistent with observable surface boulders and drilling results from the east side of Duval River (Smith and Dallimore 1981) and near the bridge (Hsieh and Tchekhovski, 2008), and from the GPR results. Estimates of thickness are unreliable due to the very high resistivity since highly resistive features tend to appear thicker than reality in inverse models (e.g., Ingeman-Nielsen, 2005). However, the observation of variable

thickness likely reflects thickening of the unit towards the fjord on the east side of the Duval River. Furthermore, Smith and Dallimore (1981) noted that the soils in this area were generally found to have low ice content, except for occasional ice rich zones within the underlying silty sand. The thickening of the very high resistivity layer could also be due to an ice rich zone within the top of the silty sand till unit. However, it is hard to generalize from point observations made in boreholes. Interesting to note is where the resistive layer outcrops in the middle of the section, marked by boulders. This corresponds to a thinner layer of alluvial deposit as shown by the underlying conductive layer. This is also observed in the GPR line where the EM signal is lost more rapidly at depths beneath the outcropping boulders (between markers F1 and F2). Additional data (Oldenborger 2010) suggest that there is significant three-dimensional heterogeneity to the subsurface near the Duval River. As mentioned above, there is an indication of more conductive material at depth (~2 kΩm CCR, ~5 kΩm GR) on the up-river part of the section and on the sections running perpendicular to the river. These are the directions in which we might expect thinning of an alluvial sheet or a low ice content of the underlying layer.

The resistivity model for the arena-campground road section (Figure 17) was difficult to interpret due to the cultural noise within the hamlet and because the true survey path along the road deviates significantly from a straight line. Nevertheless, the model shows a clear lateral transition from the alluvial fan to more conductive material that includes the effects of the roadbed and buried culverts (such as at the 90 m line position). The transition appears at the 220 m line position and is consistent with the transition at about 265 m on GPR Line A1 (the 0 m positions are not the same between the two surveys). There is not much information in the model with regards to the internal composition of the two units, however, there does seem to be a finite thickness to the fan, and there does seem to be some onlapping of conductive material onto the western shoulder of the fan.

5.2 THE SLOPING COLLUVIAL TILL TERRACE EAST OF THE DUVAL RIVER

5.2.1 CORING

Five shallow boreholes were drilled in the till terrace east of the Duval River. They revealed that the till is in general covered by a layer of colluvium or slopewash material, with local patches of peat. Examination of the core samples from the colluvial blanket down to 3 m depth indicates a sequence of coarse brown sand, gravel and pebbles, with fine sand and grey silt (Figure 18). Occasionally, buried organic layers are found in the colluvium layer, and six of them were sampled for radiocarbon dating (Table B1, Appendix B). The shape of the grains is angular. A description of the deeper soils is provided from the cuttings at DDH-01, and indicates grey silty sand. This is consistent with the findings of Smith et al. (1989) who reported that the glacial till consists of occasional cobbles and boulders in a dense matrix of silty sand.

The shallow boreholes also revealed that the thaw depth in mid-August ranged from 0.2 m to 0.72 m, with thinner active layers where peat thickness ranged from 40 to 60 cm. Below the active layer, ice lenses ranging from millimetres to centimetres in thickness are present, mostly within the fine sand and silt layers or within the peat.

5.2.2 GROUND PENETRATING RADAR

The cross-section interpreted from the major reflectors identified on the GPR profile is shown in Figure 19. The cross-section shows two different layers: the colluvial blanket of about 2 m in thickness underlain by till. The strongest reflector, which was more or less parallel to the surface, was interpreted as the stratigraphic contact between the two layers, since the thawing front was observed in the shallow boreholes to range from 0.2 to 0.72 m only. Hyperbolic reflectors more or less equally spaced within or slightly below the colluvial layer were interpreted as possible ice wedges. Ice wedges tend to refract the electromagnetic (EM) signal inside the ice wedges while oblique reflection of the EM signal is produced by the ice-wedge walls due to the range of emitting antenna (Fortier and Allard 2004). Hyperbolic reflections produced by individual boulders on the other hand are characterized by multiple hyperbolic reflections without any refraction of the EM signal (see Appendix A, Line A2 and Line A5 for boulder and ice wedge EM signals, respectively). In addition to the GPR data, several other lines of evidence support the theory that ice wedges are prevalent in this area. Many ice wedges were observed during the excavation of the current water reservoir located further west in the same terrain unit; as at the survey site, no surface expression of ice wedges such as well defined polygons was observed (Smith et al. 1989). The thick colluvial deposits tend to mask the ice wedges, which otherwise can normally be identified on aerial photographs by the presence of tundra polygons. Other GPR profiles (e.g. Line A5 - Appendix A) conducted parallel to the fjord in this area are consistent with the one presented in Figure 19. In the spring of 2010, a network of active frost cracks was observed, and ice veins were visible in the near surface in what is normally the active layer (Figure 20).

5.2.3 ELECTRICAL RESISTIVITY

Electrical resistivity data were collected along the same section as the GPR data and are shown in Figure 21. As with the GPR, the resistivity models clearly show two different layers. The resistive surface layer (~3000 Ωm CCR, ~6000 Ωm GR) is interpreted as frozen sand/silt 2-3 m thick corresponding to colluvium. Thickness is based on the CCR model, but may be over-estimated. Resolution of the electrical models is too low to allow identification of an active layer or any ice wedges. The active layer will contribute to a reduction in the bulk resistivity of the surface layer, whereas any ice wedges will contribute to an increase in the bulk resistivity. Observed small-scale heterogeneity is interpreted to be a result of ice-rich zones, particularly near SDH-20. The lower layer, interpreted as till, has low values of resistivity (~100 Ωm CCR, ~200 Ωm GR). This is consistent with the till having a dense matrix of silty sand that becomes finer with depth (Smith et al. 1989, Smith and Dallimore 1981). These values may be a result of the high conductivity of saline porewater. For instance, high salinity of porewater was measured in a till layer above the marine limit southwest of the present water reservoir (Hyatt 1992). However, due to the cold temperature of the permafrost (-7.1 °C; see below) only a very small amount of free electrolytes should be present, so clay mineralogy may be another factor affecting the conductivity. Salinity measurements of the core samples have not been done at the time of writing, but will indicate if the till contains layers of saline clay or not. There seems to be increased conductivity at depth towards the fiord, which may be related to the landfill and vehicle graveyard at the foot of the slope. Finally, at the upslope end of the section, increased resistivity may be related to high boulder occurrence, as observed in the field.

Other capacitive and galvanic surveys were performed in this area (Oldenborger 2010). All models are similar to the one presented in Figure 21. However, Oldenborger (2010) results indicate some heterogeneity in the underlying layer, with an increase in conductivity from the northeast to southwest.

5.3 A ROCKY PROMONTORY COVERED WITH MARINE SILTS AND SANDS

5.3.1 CORING

The majority of the shallow boreholes, ten in total, were drilled in the colluvium and marine sediments of Unit 4. Massive silt sediments were encountered in SDH-14, SDH-08 and SDH-10 at depths of 1 to 2 m below the surface (Figure 22a), overlain by medium to coarse brown and grey sand. At other sites, fine to coarse brown and grey silty sand with gravel were encountered (Figure 22b). One shell found between 2.37 and 2.47 m deep in borehole SDH-08, yielded a calibrated radiocarbon age of 9553 cal BP (UCIAMS-859), which is now the oldest available early Holocene radiocarbon date in Pangnirtung. Samples from paleosols and layers of organic matter within the colluvium were also collected for radiocarbon dating (Table B1, Appendix B). A well-sorted sand overlain by colluvium was found at SDH-15 and SDH-16, at depths of 2.4 and 0.3 m respectively, which is consistent with the beach deposit described by Aitken and Gilbert (1989). Bedrock was possibly encountered at 2.65 m depth at SDH-14, near the northwest end of the runway. According to Smith and Dallimore (1980), bedrock was reached in four boreholes on the southwest side of the runway located along a line running from SDH-15 to the midway point between SHD-15 and SDH-09; the depth to bedrock was 1.8, 1.5, 6.3 and 9.2 m, going from west to east. Bedrock was not encountered on the southeast side of the runway to depth of 15 m (DDH-Airport).

The thaw depth in mid-August ranged from 0.41 to 1.05 m over natural, undisturbed surfaces, but reached up to 1.8 m in gravel pads, based on the thermistor cable data (see Section 6). At many locations, ice-rich sand and gravel were observed, as were ice lenses in the upper layer of the marine silt, ranging from millimetres to centimetres in thickness. Site SDH-06, located close to the approximate southern limit of the marine sediments, is particularly ice-rich (Figure 22c), potentially a result of being located in an area where subsurface water flows in the colluvial surface layer.

5.3.2 GROUND PENETRATING RADAR

The cross-section interpreted from the GPR profile in the park area where SDH-10 is located is shown in Figure 23. Bedrock was not observed along this line even though the bedrock outcrops near the fjord, and was encountered at 6 m depth during construction of new housing to the south of this profile (Canadrill Ltd., personnal communication). The GPR signal loss in the fine sediments prevents deep signal penetration and detection of the bedrock, leading to an unknown thickness of the fine-grained marine unit. The strongest reflector, which was more or less parallel to the surface at a depth of about 2 m, was interpreted as the stratigraphic contact between the upper colluvium (mostly sand) and the lower marine sediments (silt). The thawing front shown for the length of the profile is based on a thawing front of 1 m observed at SDH-10.

The GPR signature of this unit (rapid loss of the GPR signal in the fine sediments) is similar to other GPR profiles conducted on the marine silts and sands (Lines A1, A3, A4, and A6 to A8, Appendix A). However, the contact between the colluvium and the marine sediments does not always appear clearly, as shown in Line A6 (Appendix A) between 30 and 70 m. This suggests that the thickness of the colluvium is probably variable over this terrain unit. Line A6 was conducted in the same area of the profile presented in Figure 23, but crosses SDH-10 from a slightly different angle providing a view of the spatial distribution of the colluvium.

Variability in the EM signal penetration along survey lines may be explained by coarser marine sediments, higher ice content or even occurrence of bedrock near or at the surface (Lines A6 to A8, Appendix A). In Line A7, bedrock outcrops under the road and within a few meters of the surface at around the 44, 120, 143, 225, and 265 m line positions. However, the contact is rapidly lost as it dips under the marine sediments. It is expected that the rolling bedrock topography underlying the marine sediments changes rapidly, as observed along the coastline.

5.3.3 ELECTRICAL RESISTIVITY

The electrical resistivity models for an area near SDH-10 are shown in Figure 24, and correspond to GPR Line A6. The models show a dipping contact between a resistive layer (>10 kΩm CCR and GR) that extends from the surface to approximately 2-4 m deep and a conductive lower layer (~500 Ωm CCR and GR). The GR data are not as noisy as the CCR data and result in a much cleaner model. However, the coverage associated with the deployment of a single Wenner array is limited in horizontal extent.

The shallow borehole, SDH-10, intersects a contact between sand and silt at ~2.2m depth. This is in good agreement with the location of the contact that can be inferred from the CCR model at approximately the 31 m line position. As a result, the resistivity model can be used to extend the contact northward. Based on the observed resistivities, the surface colluvium appears to be discontinuous or variable in thickness. This is consistent with the GPR results. The regions of particularly high resistivity may be associated with ice-rich sands and silts within the colluvium and the top of the marine sediments. The resistivity values of the underlying material are higher than expected for marine sediments with presumably high salt content. These values are actually higher than that of the till of colluvial terrace unit east of the alluvial fan (500 Ωm vs. 50–100 Ωm CCR).

As in the GPR profile for the same line, the surface of bedrock was not observed. Bedrock should represent a resistive anomaly unless highly fractured and saturated with unfrozen saline porewater, and we can indentify no such anomaly in the resistivity models. This again suggests extreme variability of the bedrock surface.

Other capacitive surveys were performed over the colluvium and marine sediments and in the transition zone of the southern limit of the marine sediments with the till (Oldenborger 2010). Features similar to the ones shown in Figure 24 characterize the area along the north side of the runway and up-slope on the south side of the runway. However, Oldenborger (2010) identified the

resistivity of the underlying material of the up-slope lines to be similar to the one of the till of colluvial terrace terrain unit east of the alluvial fan, and therefore, it is interpreted as a till.

6 PERMAFROST TEMPERATURES

Of the five thermistor cables installed in Pangnirtung, three are located in marine sediments (DDH-Airport, SDH-06, and SDH-14), one is located in the alluvial fan (DDH-01), and one in the till covered by colluvium to the east of the Duval River (DDH-02). At the time of writing, ground temperature data for over two years (June 2008 to mid-August 2010) was available for the airport site, and a one year record (mid-August 2009 to mid-August 2010) was available for the remaining sites (SDH-06, SDH-14, DDH-01, and DDH-02).

The ground temperature envelopes, defined by the minimum and maximum recorded temperature for each sensor, are plotted for each cable in Figure 25, as are the mean annual ground temperatures (MAGTs). The maximum thaw depth (active layer), given by the intersection between the maximum temperature profile and 0 ºC, as well as the snow thickness, observed in late March 2010, are also shown for each permafrost temperature monitoring site). At 12 m depth, the mean annual ground temperatures (MAGTs) are -2.8, -5.2, and -7.1 ºC, respectively for the sites DDH-01, DDH-Airport, and DDH-02. The depth of zero annual amplitude, below which seasonal temperature variation is negligible, is 12.3 m at the Airport site and approximately 14 m at sites DDH-01 and DDH-02. By contrast, the range in temperature at site SDH-14 indicates a smaller amplitude near the ground surface and a rapid decrease of the thermal amplitude with depth compared to other sites, resulting in an approximate depth to zero amplitude of 2.7 m. In the marine sediments, the maximum thaw depth in 2009 varies from 0.75 m (SDH-06) to 1.8 m (DDH-Airport). It is 1 m for the till (DDH-02) and 2.5 m for the alluvium (DDH-01). Snow accumulations varied from site to site, ranging from 0.16 m at the exposed DDH-02 site, to 0.20 m at both DDH-Airport and SDH-06, 0.37 m at DDH-01, and 1.23 m at the sheltered SDH-14 site.

The current results are consistent with the temperatures reported in previous studies (Isherwood and Smith 1983, Smith et al. 1989, Hyatt 1998, Hsieh and Tchekhovski 2008) with respect to the wide range of ground temperatures measured throughout the community. Specific trends in the ground temperatures are not easily discernable between the 1980's values and the current data since the measurement sites are not the same. However, past and current ground temperatures tend to indicate warmer permafrost in the vicinity of the alluvial fan and colder permafrost on both sides of it.

At DDH-01, snow accumulation was slightly higher than the more exposed sites, DDH-02 and DDH-Airport, but it is not enough to explain the difference of more than 2 and 4 ºC, respectively, at 12 m depth. The warmer ground temperatures of the alluvial fan may be explained by a higher thermal conductivity usually associated with gravelly and bouldery sand, causing this deposit to respond faster to any changes in air temperature or surface disturbances. Furthermore, Smith and Dallimore (1981) observed groundwater discharge and icings in the alluvial fan north of the old water reservoir and close to the fjord, west of the Duval River, during the summer months and into

December and January. Frozen ground was encountered in all of their boreholes in the alluvial fan sediments, although, like this study, temperatures were warmer than elsewhere in the community. Therefore, groundwater flow in the upper thawed layer may have delayed ground cooling and may have induced additional heat to flow into the deeper layers. The proximity of the Duval River to DDH-01 and the fact that the river bed was 10 m higher before June 2008 may also have contributed to warmer permafrost at depth in this location. The thick active layer is related to the coarse sediment and probably also influenced by the warmer MAGTs throughout the profile.

The cold ground temperatures at DDH-02 are due to the thin snow cover resulting from strong easterly winds (FoTenn and Trow 2007). The active layer thickness of about 1 m is related to sediment type and the cold permafrost temperatures. Similar ground temperatures are expected to prevail throughout the area of the till terrace, while active layer thickness may vary on the order of a few tens of centimetres depending on the surface conditions, thickness of the peat, and water content of the ground.

In the western part of the community, although the MAGTs are variable in the near surface, the trend of MAGTs deeper than those measured at sites SDH-06 and SDH-14 is similar to the ones observed at the Airport site (see Figure 25). Therefore, a MAGT of -5.2 ºC at a depth of 12 m seems to be a reasonable estimate to characterize areas of marine sediments over bedrock. The narrow thermal amplitude and the expected shallow depth of zero annual amplitude at SDH-14 is probably explained by the nature of the sediments (fine grained from almost the surface down to 2.7 m), a higher water content (to be confirmed by laboratory analysis), and thicker snow cover (about 1.23 m), resulting in warmer ground temperature profiles during the winter. Unlike sites SDH-06 and SDH-14, the Airport site is on a gravel pad, where heat from the air is transferred to the surface with little interference, resulting in a thicker active layer. In addition to summer air temperature being the primary factors to explain active layer depth, snow cover from the previous winter can also contribute to a deeper thaw depth (L'Hérault 2009). For example, if the snow cover in 2009 was similar to that observed in 2010, the thicker snow cover of 1.23 m at SDH-14 compared to the 0.20 m at SDH-06 would likely explain the difference in the active layer thicknesses. Greater peat content was also observed near the surface at SDH-06. Therefore, active layer thickness throughout the marine unit will vary significantly depending on local surface conditions.

7 GROUND SURFACE TEMPERATURES

Ground surface temperatures complement the ground temperatures at depth. Data from the first year of record are summarized in Table 1 (mid-August 2009 to mid-August 2010). Air thawing and freezing indices for the same period are respectively 834 and 2988.7 degree days and were used for the calculation of surface thawing and freezing n-factors.

In general, high values of surface thawing indices (or surface thawing n-factor) will correspond to a thicker active layer, while low values of surface freezing index (or surface freezing n-factor) will indicate warmer MAGTs. Under natural ground surface conditions, the surface thawing n-factors are

less variable than the surface freezing n-factors. For the thawing n-factors, this is probably due to the similar sediment type at the near-surface, usually sands, and the dryness of most of the surfaces. For the freezing n-factor, it is likely due to the local variation in snow cover and density; thick snow cover and low density will enhance the insulation capacity of the snow.

The alluvial deposit (st-4 and st-5) is the only terrain unit with a thawing n-factor above 1, which is consistent with the thicker active layer observed at DDH-01. No difference is expected between the ground surface thermal regime on the alluvial bars (st-4) and in the depressions of old channels (st-5). The sensor showing the lowest surface thawing n-factor of 0.79, st-7, was originally buried under wet vegetation cover which usually provides less insulation than dry vegetation. However, the temperature sensor at this location was found in August 2010 floating in a small shallow pond. Thus, these surface temperature measurements in summer time are not representative of the ground surface. The lowest surface freezing n-factor of 0.25 (st-2) is well explained by the snow cover of over 1 m, while the highest value of 0.82 (st-8) is characteristic of thin snow cover. The gravel road (st-6) shows the highest surface thawing and freezing n-factors of all sites due to the bare surface of sand and gravel, and the absence of a snow cover. It is important to note that the values in Table 1 are calculated from only a short period of record and there will likely be inter-annual variability.

8 SIGNIFICANCE OF THE RADIOCARBON DATING RESULTS OF BURIED ORGANICS IN THE SURFACE COLLUVIUM LAYER

Figure B1 (Appendix B) shows the location of drill holes where buried organic layers where found and sampled in the colluvium layers over till and marine sediments (Carbonneau, in prep.). Table B1 (Appendix B) show the ages for those samples obtained by radiocarbon dating. These results show that diffuse surface flow over the frozen terrain surface has been ongoing for the past 6000 years. During snow melt, the water flows over the sloping terrain in multiple, diffuse, water tracks. The main impact of this process over time has been the buildup of ice-rich permafrost in the top 2 m of the ground through the accumulation of wet colluvium. Another implication is that the terrain is now sensitive to disturbances from surface flow that is modified from diffuse to concentrated, e.g. into ditches or gullies, which would provoke some thermal erosion.

9 PERMAFROST SENSITIVITY TO WARMING

The information acquired from this project to date provides insight into the sensitivity of the local permafrost to warming. New knowledge on ground temperatures as well as on snow conditions, surficial deposits, geotechnical properties, ground ice contents and geomorphic processes now provides a better assessment of terrain sensitivity and hazards. The interpretation of the maps and

data obtained so far demonstrates spatial variations in permafrost properties related to the nature of surficial deposits and geomorphic processes that have been active for a long time.

a) Ground ice and permafrost temperature

It generally appears that colluvium deposition on the terrain surface, linked to surface water flow on an impervious ground at snowmelt and during heavy rain events, has produced a layer of ice-rich permafrost near the surface of the ground over large areas of the community. Indeed, ice rich colluvium is found in almost all shallow boreholes, with the exception of the bouldery material of the alluvial fan. Furthermore, in areas of marine sediment, this colluvium overlies marine silts that are still richer in segregation ice down to depths of 2-3 m. Thawing of ice-rich permafrost can lead to ground instability and weakening of bearing strength. For the marine sediments overlain by colluvium, this may result in thaw settlement and increased soil creep. As an example, the garage on the east side of SDH-06 which is built on a concrete floor underlain by ice-rich permafrost shows signs of thaw settlement as evidenced by its sagging centre. In general, the high salinity of marine sediments can be a concern because of the increased sensitivity to small changes in temperature; this is especially important for infrastructure built on piles. However, this may not be the case in Pangnirtung as the high resistivity values encountered during the geophysical surveys indicate that the marine sediments are not highly saline. In addition, the marine sediments are not believed to form a continuously thick deposit since bedrock outcrops near the fjord and was encountered within 10 m of the surface during drilling (Canadrill Ltd., personal communication, and result of SDH-14), except on the southeast side of the runway (Smith and Dallimore, 1980, and result of DDH-Airport). Therefore, the ability to drive piles to bedrock would limit the effect of any loss of ground strength or settlement as a result of warming permafrost. This may not be the case in the vicinity of the schools and to the east of them, where little information is known about the depth to bedrock. Even if ice-rich permafrost and fine-grained material were to exhibit a greater physical response to warming (i.e. thaw settlement), the rate of these changes will be slowed by the amount of latent heat needed to melt the ground ice and by the thermal properties of fine-grained material. The current ground temperatures of this area are still sufficiently below 0ºC and warming of the MAGT at a depth of 10 to 15 m to the melting point could take more than a half of century (e.g. Delisle 2007). However, extreme events or air temperatures higher than usual (e.g. high than average years and summers leading to increased active layer depth) always have the potential to cause rapid permafrost degradation at the near surface. Local variation in snow thickness due to the prevailing wind direction (natural snow accumulation is mostly on the west side of buildings) and the municipal snow clearing practices (i.e. snowblowing) also contribute to warmer ground, making it more prone to thaw. For instance, at site SDH-14, warm permafrost (about 0.6 to 0.9 ºC) occurs at a depth of 2 m under a thick snow cover.

Because of the current warm thermal state of the alluvial fan and the fact that coarse-grained material exhibits a greater thermal response to changes in air temperature, the ground thermal regime of this area is expected to respond more rapidly to climate warming than any other material throughout the community, with the exception of bedrock. However, the combination of relatively permeable coarse-grained material and low ice content will result in good drainage and stable ground when

thawed, and therefore, the mechanical response of this unit to warming should be minimal, even if its thermal response is high.

The coldest permafrost of the four main units is found in the till terrace on the east side of the community where the current municipal expansion is taking place. The main contributing factors to the colder temperatures are likely peat and snow cover. Insulation by the peat, which seems to be generally thicker in this area, provides a good thermal buffer against warm summer air temperatures at locations where the peat remains dry, thus preventing the ground from warming. The thin, compact snow cover facilitates loss of ground heat, keeping the permafrost cold in winter. The cold temperature of the permafrost of this area will probably delay the impact of warming on the permafrost, similar to the situation on the west side of the hamlet. However, any new development in this area will eventually modify the ground surface conditions by altering the snow distribution pattern, and disturbing the vegetation cover and the natural surface drainage. As a result, the ground may warm, even if the air temperatures remain the same. The likely presence of a network of ice wedges in this area, and also the probable presence of undetected ice-wedges elsewhere in town, must be kept in mind. Those ground ice forms could be dramatically eroded by surface water flow in frost cracks, leading to intense tunnelling and gullying and major terrain disruption (Fortier et al. 2007). This could happen as a result of significant snowmelt or rain events. Care is necessary in planning urban drainage and locating culverts in order to avoid excessive concentration of surface water flow that would eventually be channelled into ice-wedge troughs. Such thermal erosion and gullying would be a change in the natural processes of highly dispersed surface water flow that has been ongoing for the past 5000 years as evidenced by the radiocarbon dating of buried organic layers by colluviums accumulation (Table B1, Appendix B).

b) Thermal erosion by the Duval River

The alluvial fan and the river bed are underlain by till which has a fine-grained matrix. During the June 2008 flood, the high velocity and the heat of the water easily eroded the river bed and the underlying till, leading to the collapse of large areas of the terrace bordering the Duval River. It is likely that the warmer temperature of the permafrost near the river makes it more prone to thermal erosion since a lower heat transfer from the river water is needed to thaw the ground. Closer to the river, the ground temperature is probably warmer than that measured at DDH-01, especially where snowdrifts occur. Several snowdrifts up to nearly 3 m high were observed along the river banks (Figure 26) at the end of March 2010. Icings, flowing water from the ground that freezes on contact with air, were observed at several locations along the river. This indicates that permafrost temperatures are close to 0 °C along the river bank. This area immediately next to the river currently represents the highest geological risk in the community. Another aspect to be considered is the impact of climate change on the hydrological regime of the river. Recent mapping of the river basin shows that the small glaciers at the head of the basin are melting rapidly (Falardeau-Marcoux 2010). At the same time, the increase in active layer thickness of the tills in the basin will allow for greater water storage, leading to generally diminished flows in summer. Monitoring precipitation and basin hydrology would be important, both for better assessing the risk of thermo-erosion events during

peak flows at snowmelt and for adopting a safe strategy for ascertaining the drinking water supply of the community during dry periods.

10 CONCLUSIONS

At a time when the community of Pangnirtung needs more space for its expansion and when the climate is warming, greater care than in the past must be given to permafrost conditions and sensitivity. This statement applies as well to other Arctic communities.

Several studies and reports comment on permafrost and related features in the area of Pangnirtung (e.g. Hyatt 1990, 1992, 1998, Hyatt et al. 2003, Smith and Dallimore 1980, 1981, Hsieh and Tchekhovski 2008). Many are from the private sector and are not easily available to current land use planners, engineers and stakeholders. When available, these reports often provide relevant information on permafrost; however, their evaluation of the geotechnical properties generally rely on poor quality drill logs produced with non-coring machinery. In addition, the studies are usually project specific and therefore the results are rarely of a scale suitable for community planning. This research therefore aims to provide a comprehensive understanding of the current permafrost conditions in Pangnirtung in order to assess its sensitivity and the landscape hazards related to climate change and human disturbances. The methods applied in the field, including detailed mapping of the surficial geology, shallow and deep drilling, sampling, shallow geophysical surveys and ground thermal and snow thickness and density measurements, have proven to be an efficient way to achieve these goals.

Four main areas of Pangnirtung were recognized, based on the four dominant terrain units: 1) the alluvial fan through which the Duval River flows, 2) the alluvial terrace with boulders and eroded channels along the banks of the Duval River, 3) the till terrace overlain by colluvium to the east of the alluvial fan, also understood to be the next development area, and 4) the marine sediments overlain by colluvium to the west of the alluvial fan. Results show the distribution of ice-rich permafrost as it relates to the surficial geology; the estimated thickness of the surficial geology units, and the ground thermal regime corresponding with each terrain type. The difference in sediment types, ice content and ground temperatures will eventually lead to spatially variable thermal and physical responses of the permafrost to climate warming or to any human disturbances.

Results of this report contribute to the main goal of this project which is to support decision-making processes in community planning. However, preliminary findings which have some bearing on construction and land management practices will have to be further verified through detailed data compilation including laboratory analysis of the permafrost cores (ice and water contents, salinity, grain size, and Atterberg limits). Landscape features such as ice wedge polygons and gelifluction lobes, and surface conditions such as drainage patterns will be added to the surficial geology. Topography will be include as well, to facilitate the analysis of dynamic processes in their context and as a support tool for land management and decision making. The hydrological regime of the Duval

River and its potential for triggering thermal erosion events is also being studied in more details as it is the primary landscape hazard in the community. The data compilation and detailed study of the Duval River dynamics are the subject of two master theses (Carbonneau, in prep. and Gosselin, in prep.).

11 ACKNOWLEDGEMENTS

Support for this project was provided by Natural Resources Canada (NRCan) and the Canada-Nunavut Geoscience Office (CNGO). The DEM and the Quickbird satellite imagery were supplied by the Government of Nunavut; special thanks go to R. Chapple. Thanks also to A. Dyke (NRCan) for his initial work on surficial geology. The authors wish to thank the members of the community of Pangnirtung for their interest in the project and their knowledge of the landscape, the Hamlet office and the Senior Administrative Officer, R. Mongeau, for logistical support, and Jimmy Uniushagak and Noah Maniapik for their helpful assistance in making the fieldwork a success. Finally, Nicole Couture is thanked for her helpful comments in the review of this manuscript.

12 REFERENCES

ACIA, 2005. Arctic Climate Impacts Assessment. Cambridge University Press, 1046 pp.

Aitken, A. E. and Gilbert, R., 1989. Holocene nearshore environments and sea-level history in Pangnirtung Fjord, Baffin Island, N.W.T., Canada, *Arctic and Alpine Research*, 21(1), 34-44.

Allard, M., Fortier, R., Duguay, C., and Barrette, N., 2002. A Trend of Fast Climate Warming in Northern Quebec Since 1993, Impacts on Permafrost and Man-made Infrastructures, American Geophysical Union, Fall Meeting, abstract B11E-03.

Allard, M., Lévesque, R., Séguin, M. K., and Pilon, J. A., 1991. Les caractéristiques du pergélisol et les études préliminaires aux travaux de génie au Québec nordique. Texte préliminaire, Centre d'études nordiques, Université Laval, Québec.

Calmels, F., Gagnon, O., and Allard, M., 2005. A Portable Earth-drill System for Permafrost Studies, *Permafrost and Periglacial processes*, 16, 311–315.

Carbonneau, A.-S., in prep. Évolution géomorphologique holocène et caractérisation du pergélisol dans la communauté de Pangnirtung, île de Baffin, Nunavut. M.Sc thesis. Department of Geography, Laval University, Quebec, Quebec.

Delisle, G., 2007. Near-surface permafrost degradation: How severe during the 21st century?, *Geophysical Research Letters*, 34, L09503, doi:10.1029/2007GL029323.

Dyke, A. S., 1977. Quaternary geomorphology, glacial chronology, and climatic and sea-level history of southwestern Cumberland Peninsula, Baffin Island, Northwest Territories, Canada. Ph.D. thesis, University of Colorado, Boulder, 182 pp.

Dyke, A. S., 1979. Glacial and sea-level history of southwestern Cumberland peninsula, Baffin Island, N.W.T., Canada *Arctic and Alpine Research*, 11(2), 179-202.

Dyke, A. S., in press, Surficial geology, Pangnirtung South, Baffin Island, Nunavut. Geological Survey of Canada, Geoscience Map-P19, scale 1:100 000.

Ednie, M., and Smith, S. L., 2010. Establishment of Community-based Permafrost Monitoring Sites, Baffin Region, Nunavut, *6th Canadian Permafrost Conference*, 1205-1211.

Environment Canada, 2009. The climate normals of Canada. http://www.climate.weatheroffice.gc.ca/climate_normals/stnselect_e.html. Accessed March 15, 2010.

Falardeau-Marcoux, C. 2010. Hydrogéomorphologie du bassin versant de la rivière Duval à Pangnirtung, Île de Baffin, Nunavut. Université Laval, Mémoire de baccalauréat, Québec. 73 p.

Fortier, D. and Allard, M., 2004. Late Holocene syngenetic ice-wedge polygons development, Bylot Island, Canadian Arctic, Archipelago. *Canadian Journal of Earth Sciences*, 41: 997–1012.

Fortier, D., Allard, M. and Shur, Y., 2007. Observation of rapid drainage system development by thermal erosion of ice wedges on Bylot Island, Canadian Arctic Archipelago. Permafrost and Periglacial Processes, 18:229-243.

Fotenn and Trow, 2007. Final Background Report Pangnirtung Community Plan and Zoning By-law Update. Community and Government Services, Government of Nunavut and Hamlet of Pangnirtung, 48 pp.

Goodrich, L. E., 1982. The influence of snow cover on the ground thermal regime. Canadian Geotechnical Journal 19: 421-432.

Gosselin, P., in prep. Érosion thermique du pergélisol en milieu fluvial arctique. Dynamique des crues de la rivière Duval, Pangnirtung, île de Baffin. M.Sc thesis. Department of Geography, Laval University, Quebec, Quebec.

Hegginbottom, J. A., Dubreuil, M. A., and Harker, P. T., 1995. Canada, Permafrost. *National Atlas of Canada.* 5th ed., Natural Resources Canada, MCR 4177.

Hsieh, E. T. and Tchekhovski, A., 2008. Geotechnical Investigation and Foundation Design Recommendation, New River Bridge, Pangnirtung, Nunavut, AMEC Earth and Environmental.

Hyatt, J. A., Michel, F. A., and Gilbert, R., 2003. Recognition of subglacial regelation ice near Pangnirtung, Baffin Island, Canada. Proceedings of 8th International Conference on Permafrost. Edited by M. Phillips, S.M. Springman, and L.U. Arenson. Zurich Switzerland. A.A. Balkema, 1: 443-448.

Hyatt, J. A., 1998. Ground thermal regimes at a large earthwork reservoir on Baffin Island, Nunavut, Canada. *Seventh International Conference on Permafrost.* Edited by A.G. Lewkowicz and M. Allard. Yellowknife NWT. Collection Nordicana 57: 479-486.

Hyatt, J. A., 1992 Cavity Development in ice-rich permafrost, Pangnirtung, Baffin Island, Northwest Territories. Permafrost and Periglacial Processes, 3: 293-313.

Hyatt, J. A., 1990. Reconstruction of Holocene periglacial environments in the Pangnirtung area based on ice wedge characteristics. Proceedings of the Fifth Canadian Permafrost Conference. Edited by M.M. Burgess, D.G. Harry and D.C. Sego. Quebec City. Collection Nordicana, 54: 17-21.

Ingeman-Nielsen, T., 2005. Geophysical Techniques Applied to Permafrost Investigations in Greenland, Ph.D., Technical University of Denmark.

IPCC, 2007. Climate change 2007: the Physical Science Basis. Contribution of Working Group I to the Fourth Assessment Report of the Intergovernmental Panel on Climate Change. Solomon, S., D. Qin, M. Manning, Z. Chen, M. Marquis, K. B. Averyt, M. Tignor, and H. L. Miller (editors). Cambridge University Press, Cambridge, UK and New-York, NY, USA., 996 pp.

Isherwood, A. E. and Smith, L. B., 1983. New Pangnirtung water reservoir, detailed geotechnical investigation, Thurber Consultants Ltd., Calgary, Alberta.

L'Hérault, E., 2009. Contexte climatique critique favorable au déclenchement de ruptures de mollisol dans la vallée de Salluit, Nunavik. M.Sc. thesis. Department of Geography, Laval University, Quebec, Quebec, 161 pp.

Masterton, J. M. and Findlay, B. F., 1976. The climate of Auyuittuq National Park, Baffin Island, Northwest Territories, Atmospheric Environment Service Canada, 104 pp.

Maxwell, J. B., 1980. The Climate of the Canadian Arctic Islands and adjacent waters, Volume 1, Atmospheric Environment Service, Canada, 532 pp.

Moorman, B. J., Robinson, S. D. and Burgess, M. M., 2003. Imaging Periglacial Conditions with Ground-penetrating Radar. Permafrost and Periglacial Processes, 14: 319-329.

Oldenborger, G. A., 2010. Electrical Geophysics Applied to Assessing Permafrost Conditions in Pangnirtung, Nunavut, *Geological Survey of Canada Open File* 6725, 39 pp.

Pearson, C., Murphy, J., Halleck, P. Hermes, R., and Mathews, M., 1983. Sonic and resistivity measurements on Berea sandstone containing tetrahydrofuran hydrates: a possible analog to natural gas hydrate deposits. *Fourth International Conference on Permafrost* , Fairbanks, Alaska, National Academy Press, Washington D.C., 973-978.

Pullan, S. E., Hunter, J. A., and Gilbert, R., 1983. A shallow seismic survey on the intertidal flats at Pangnirtung, Baffin Island, Northwest Territories, *Geological Survey of Canada Current Research*, 83-1B, 273-277.

Smith, L. B., Notenboom, W. G., Campbell, M., Cheema, S., and Smyth, T., 1989. Pangnirtung water reservoir: geotechnical aspects. Canadian Geotechnical Journal, 26: 335-347.

Smith, L. B. and Dallimore, S. R., 1981. Pangnirtung land assembly geotechnical investigation, Thurber Consultants Ltd. Edmonton, Alberta.

Smith, L. B. and Dallimore, S. R., 1980. New Pangnirtung water reservoir preliminary geotechnical investigation, Thurber Consultants Ltd. Edmonton, Alberta.

Smith, S. L., Burgess, M. M., Riseborough, D. W., and Nixon, F. M., 2005. Recent Trends from Canadian Permafrost Thermal Monitoring Network Sites, *Permafrost and Periglacial Processes*, 16: 19-30.

Smith, S. L., Romanovsky, V. E., Lewkowicz, A. G., Burn, C. R., Allard, M., Glow, G. D., Yoshikawa, K. and Throop, J., 2010. Thermal state of permafrost in North America – A contribution to the international polar year. Permafrost and Periglacial Processes, 21: 117-135.

Throop J., Smith, S. L., and Lewkowicz, A. G., 2010. Observed recent changes in climate and permafrost temperatures at four sites in northern Canada, *6th Canadian Permafrost Conference*, 1265-1272.

Site	Sensor depth below ground surface (cm)	MAGST (°C)	Thawing Degree Days	Freezing Degree Days	Thawing n-factor	Freezing n-factor	First day ground temperature continuously below 0°C	First day ground temperature continuously above 0°C	Snow depth (cm)	Average snow density (g/ccm)	Date of snow depth measurement	General location	Surface condition at time of installation (Aug-09)	Vegetation
st-1	2	-1.94	728.3	1435.3	0.87	0.48	23-Sep-09	10-May-10	30	0.154	26-Mar-10	Near SDH-06, south side of airport	Dry to moist	Grasses
st-2	2	0.03	766.5	756.4	0.92	0.25	23-Sep-09	24-May-10	123	0.283	24-Mar-10	Near SDH-14, north of airport right-of-way	Moist	Grasses
st-3	2	-2.70	724.6	1711.5	0.87	0.57	22-Sep-09	14-May-10	20	0.369	24-Mar-10	In open area, near playground and RCMP building	Dry	Grasses
st-4	2	-3.52	942.2	2227.7	1.13	0.75	1-Oct-09	14-May-10	21	0.255	23-Mar-10	On alluvial fan, west of DDH-01	Dry	Grasses
st-5	2	-3.56	949.5	2249.2	1.14	0.75	30-Sep-09	14-May-10	37	0.498	23-Mar-10	On alluvial fan in small depression between alluvial bars, near DDH-01	Dry	Grasses & low shrubs
st-6	15	-4.84	1262.5	3029.2	1.51	1.01	1-Oct-09	8-May-10	-	-	-	In road embankment near the Government of Nunavut building	Dry	Bare/gravel
st-7	2	-3.36	661.4	1886.7	0.79	0.63	25-Sep-09	14-May-10	22	0.307	24-Mar-10	In a small depression, in open area behind the GN building	Wet	Grasses
st-8	2	-4.45	824.9	2449.9	0.99	0.82	23-Sep-09	14-May-10	1	-	24-Mar-10	In a small hummock, near a row house unit, on the east side behind GN building	Dry	Grasses
st-9	2	-4.46	785.6	2413.3	0.94	0.81	23-Sep-09	14-May-10	16	0.200	24-Mar-10	On washed till terrace, near DDH-02	Dry	Mosses

Table 1: Summary of the ground surface temperatures. See Figure 2 for site locations.

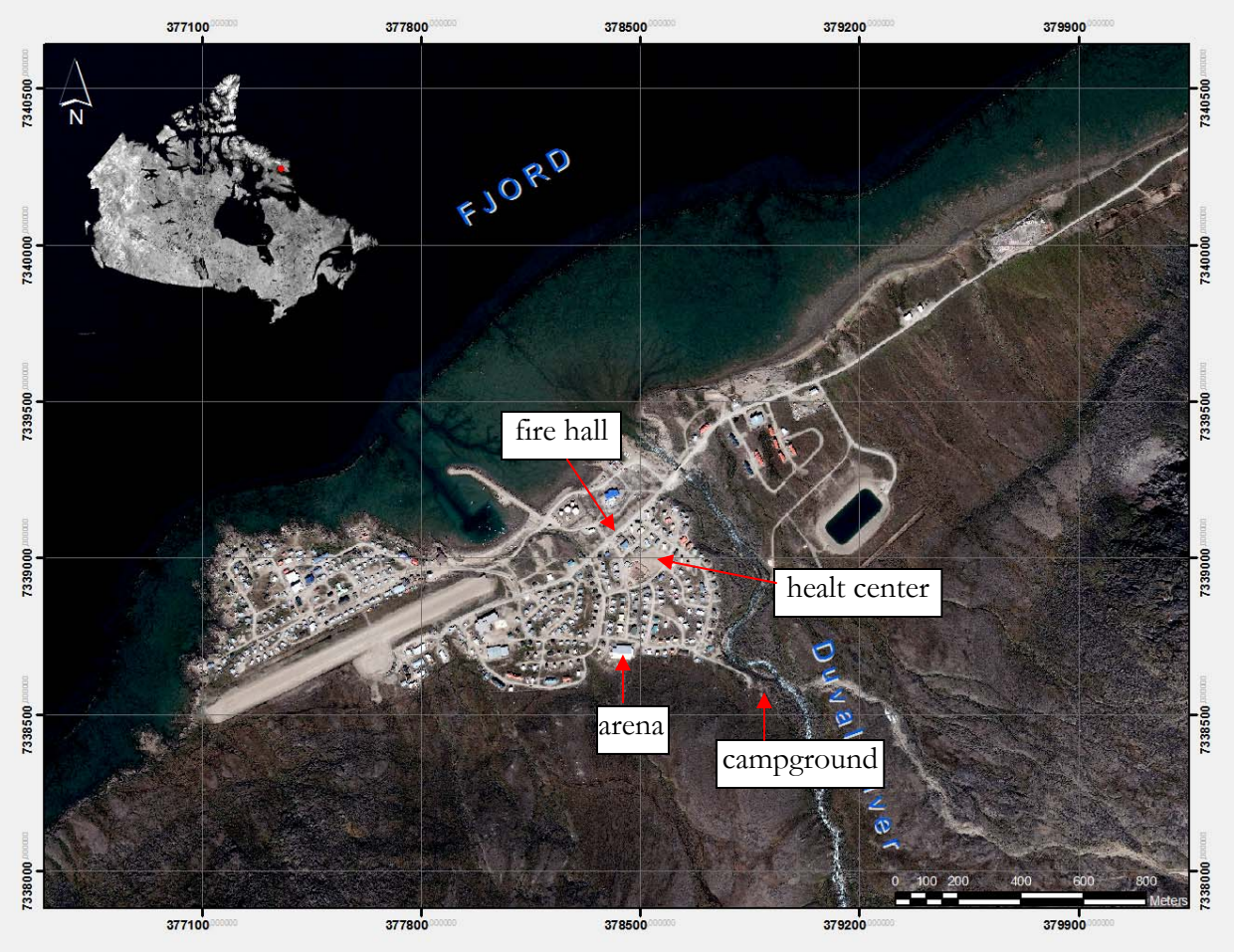

Figure 1: Location of the study site, Pangnitung, Nunavut. Background image (Quickbird), Includes copyrighted material DigitalGlobe, Inc., all rights reserved.

Figure 2: Summary of the summer 2009 field work. Location of boreholes, thermistor cables, air and ground surface temperature sensors and geophysical surveys. Background image (Quickbird), Includes copyrighted material DigitalGlobe, Inc., all rights reserved.

Figure 3: Shallow drilling with the portable earth drill.

Figure 4: Deep drilling with the airtrack drill.

Figure 5: Thermistor cable and data logger in a PVC casing for permafrost temperature monitoring.

Figure 6: Miniature data logger (HOBO) used to record ground surface temperatures.

Figure 7: Location of miniature temperature loggers, st-1 to st-9. Background image (Quickbird), Includes copyrighted material DigitalGlobe, Inc., all rights reserved.

Figure 8: Snow depth and density measurements.

Figure 9: Ground penetrating radar (GPR) unit by Sensors and Software Inc. showing the antennas mounted on the cart.

Figure 10: The capacitively-coupled resistivity (CCR) OhmMapper composed of a coaxial-cable array with one transmitter and several receivers that are pulled along the ground.

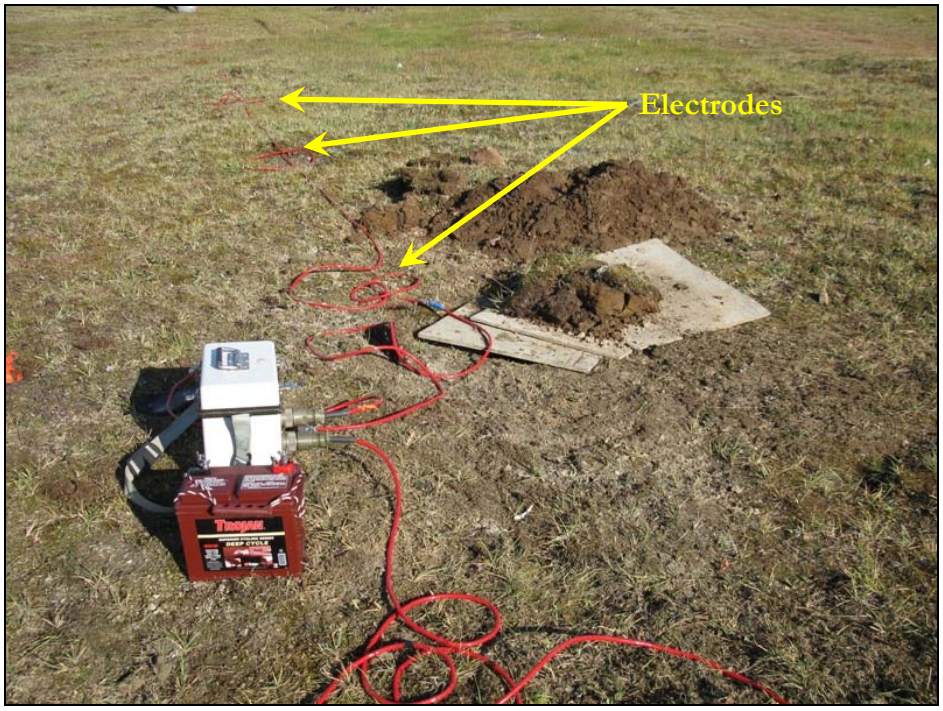

Figure 11: The galvanic resistivity (GR) system consists of a resistivity meter (IRIS Syscal R1+ Switch 48) and electrodes hammered into the ground and connected by cables laid out along a survey line.

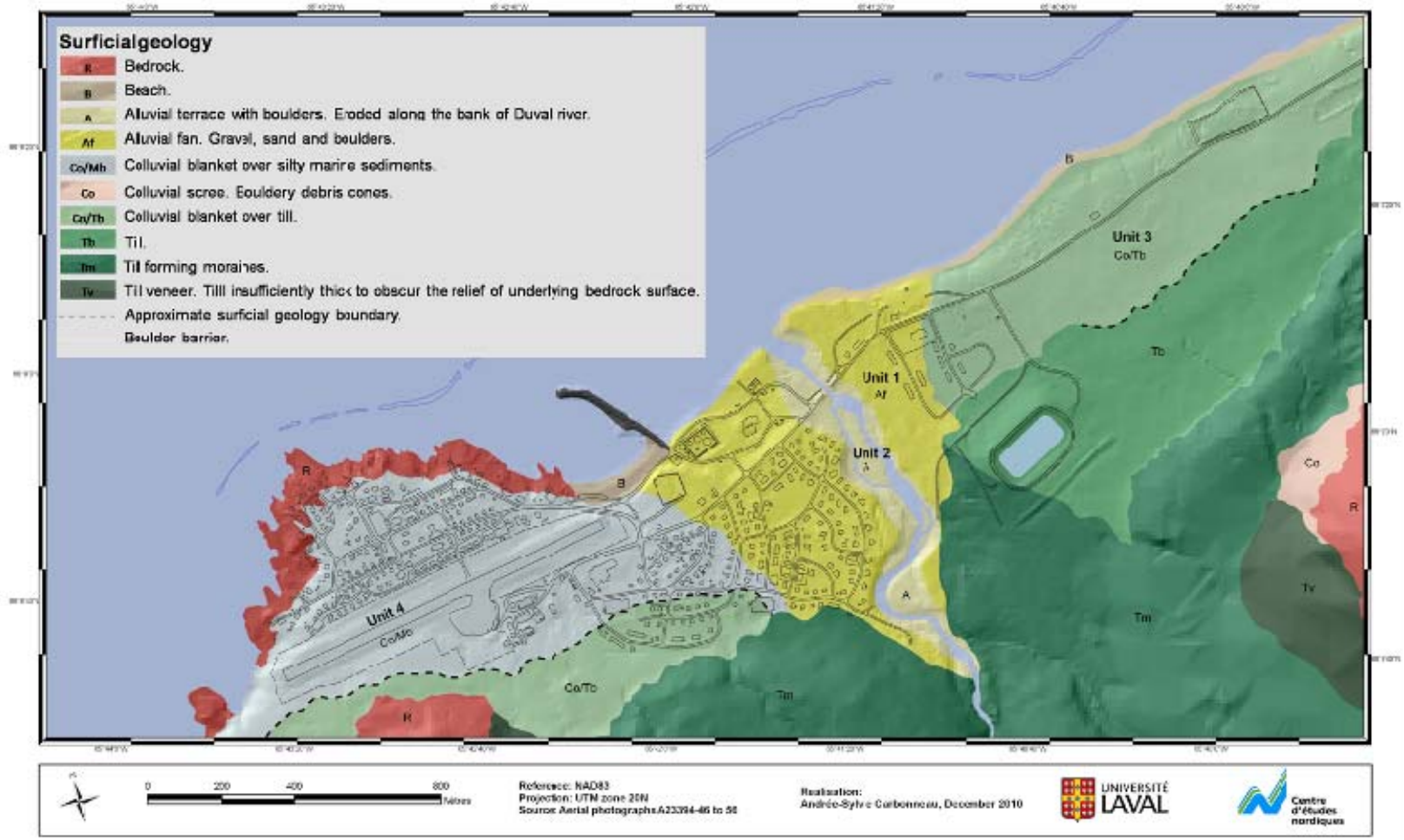

Figure 12: Surficial geology map of Pangnirtung. Infrastructure is located on four major units: 1) the Holocene debris fan of the Duval River, 2) the alluvial terrace with boulders and eroded channels along the banks of the Duval River, 3) the sloping terrace covered by colluvium to the east of the Duval River, and 4) the rocky promontory covered with marine silts and sands.

Figure 13: Stratigraphic section along the west bank of the Duval River; the upper boulder layer is 3 m thick and overlies till. See Figure 2 for site location.

Figure 14: Permafrost core sample taken in an old alluvial channel (SDH-19). See Figure 2 for site location.

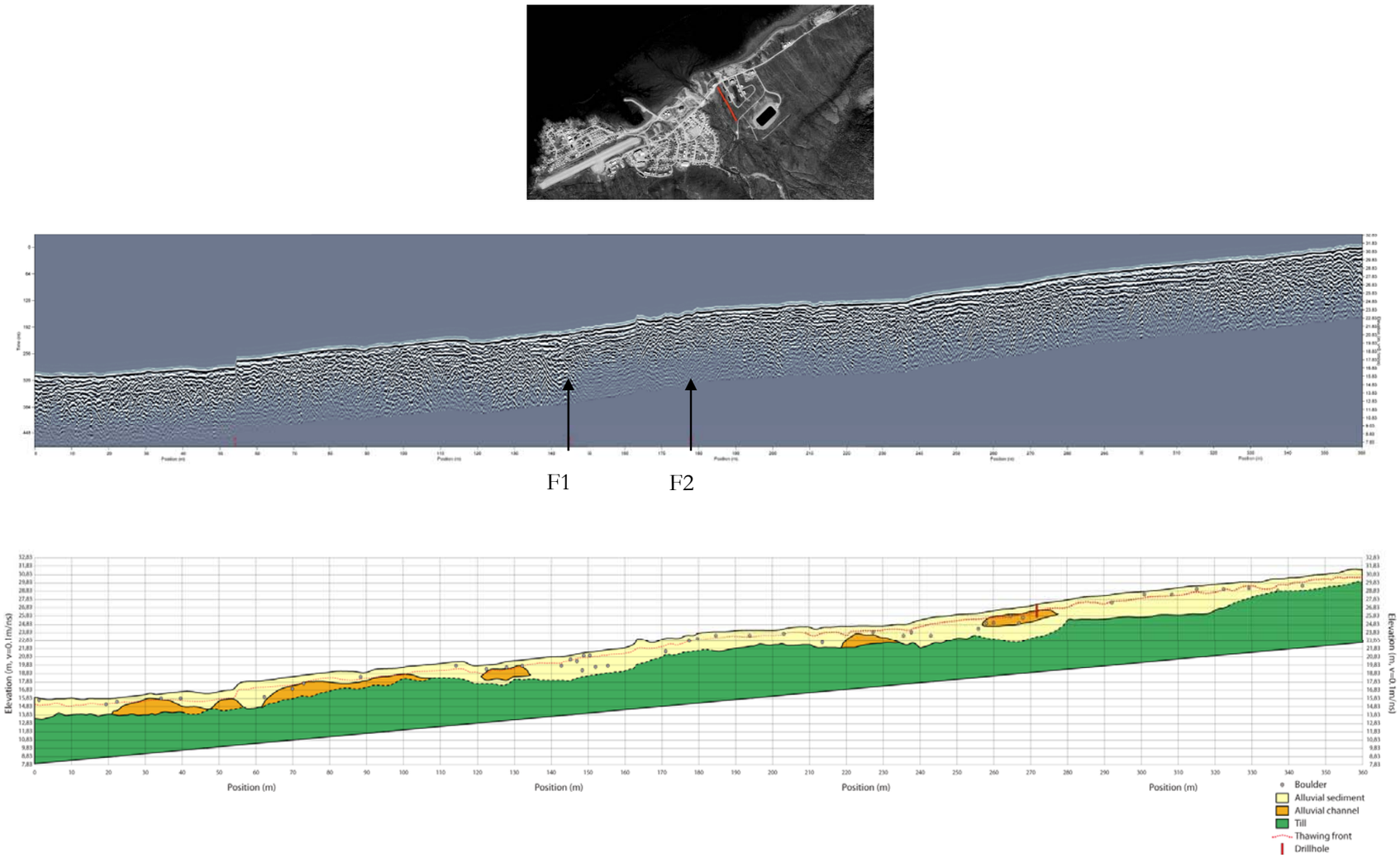

Figure 15 : GPR profile and interpreted cross-section along the Duval River show the stratigraphic contact between the alluvial sediments and the underlying till. The more or less parallel reflector between 0.75 and 1 m was interpreted as the thawing front. Between markers F1 and F2, the EM signal is lost more rapidly at depths beneath the outcropping boulders.

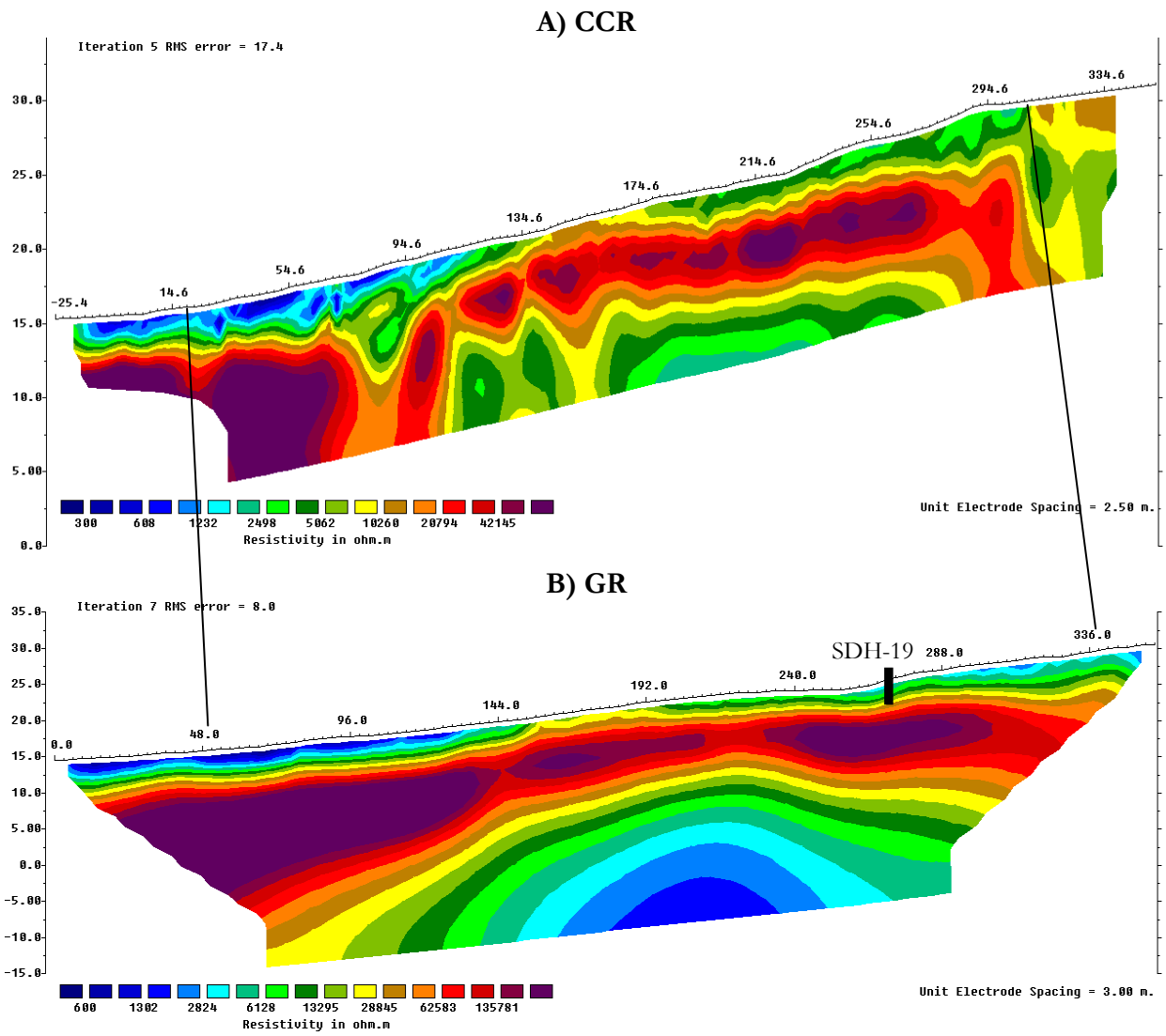

Figure 16: A) CCR and B) GR resistivity models along the Duval River section. Note that horizontal scales are different and the 0 m position on the GR section corresponds to approximately -28 m on the CCR section.

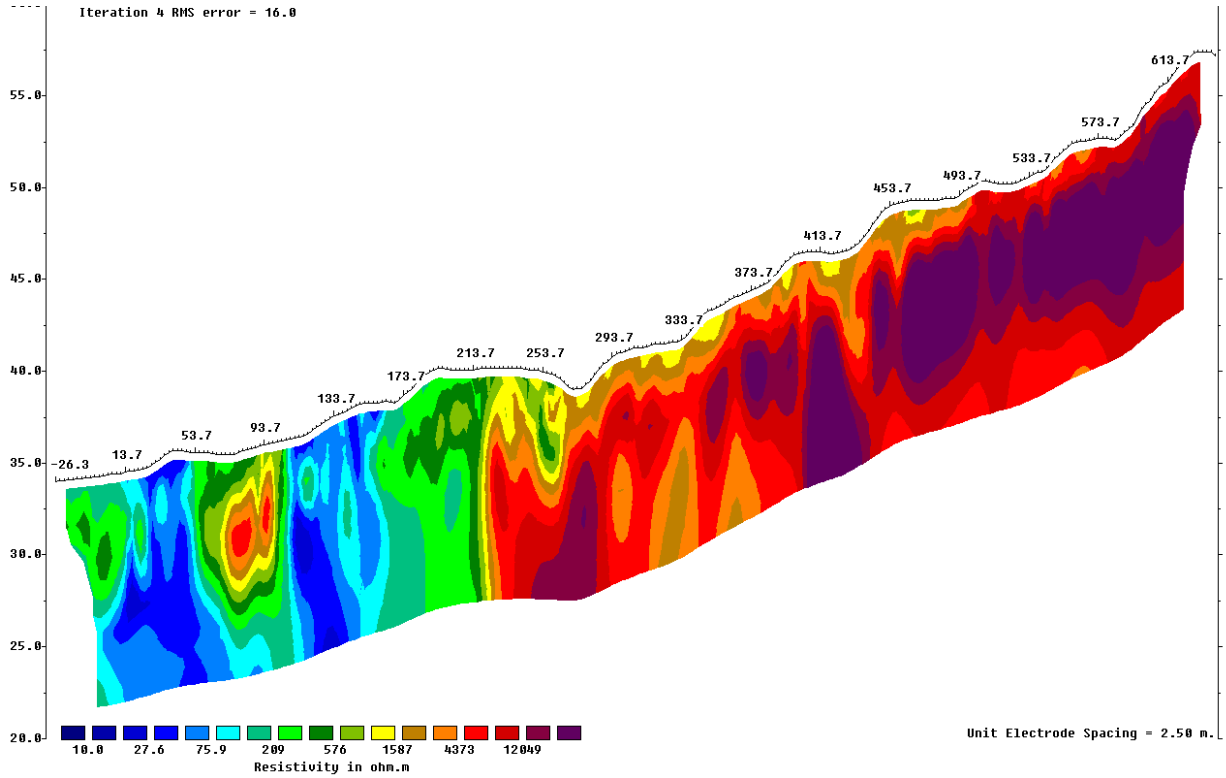

Figure 17: CCR resistivity model along the arena-campground road.

Figure 18: Permafrost core sample taken in the colluvial blanket (SDH-20). See Figure 2 for site location.

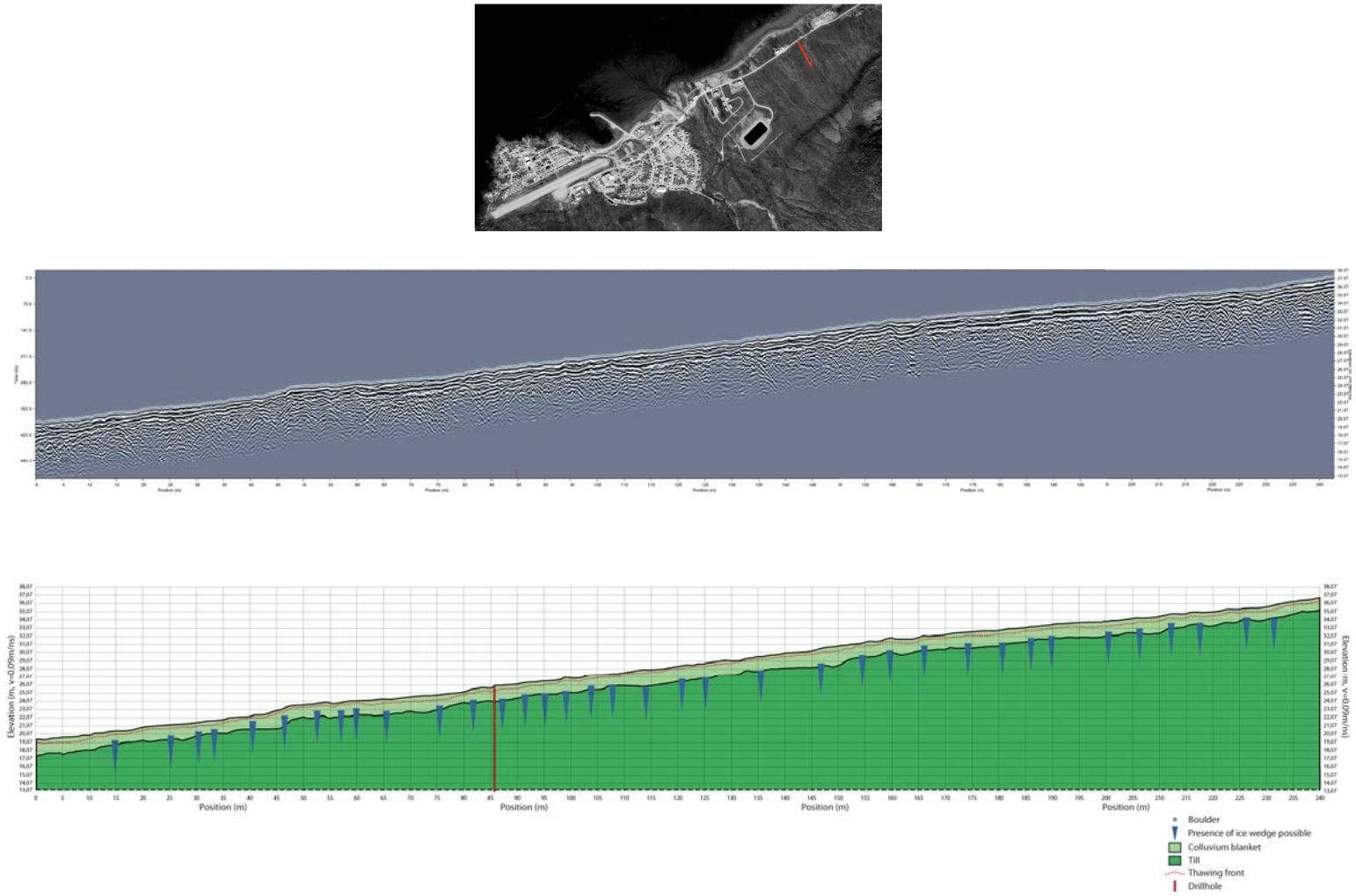

Figure 19 : GPR profile and interpreted cross-section along the till terrace east of the Duval River show the colluvial blanket deposit of about 2 m thick underlain by a till deposit. Hyperbolic reflectors more or less equally spaced within the colluvial layer or slightly below the stratigraphic contact were interpreted as ice wedges.

Figure 20 : A) Network of active frost cracks observed along the till terrace east of the Duval River and B) Plan view of visible ice vein in the near surface in what is normally the active layer.

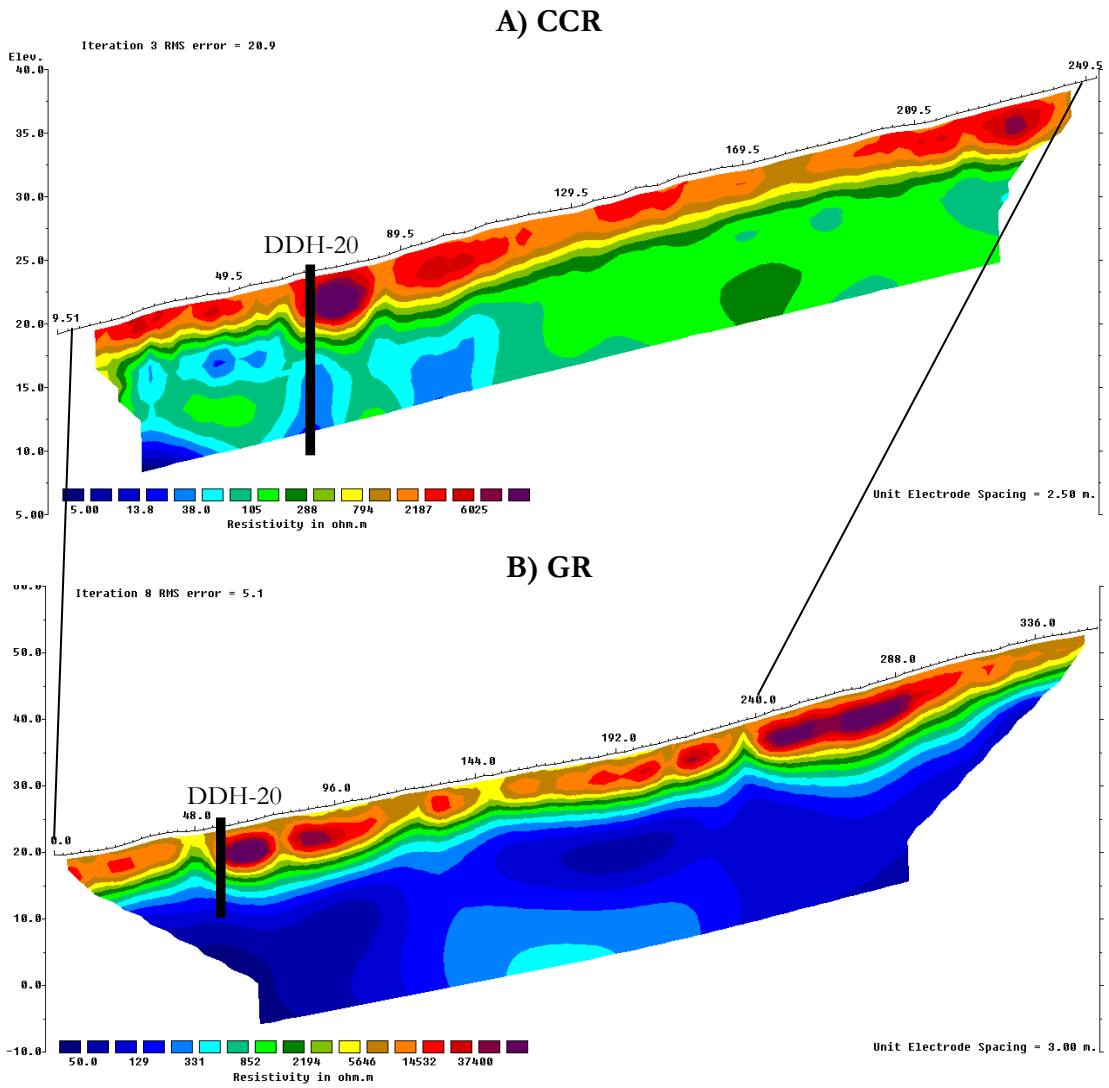

Figure 21 : A) CCR and B) GR resistivity models along the till terrace section. The 0 m position on the GR section corresponds to approximately 12 m on the CCR section.

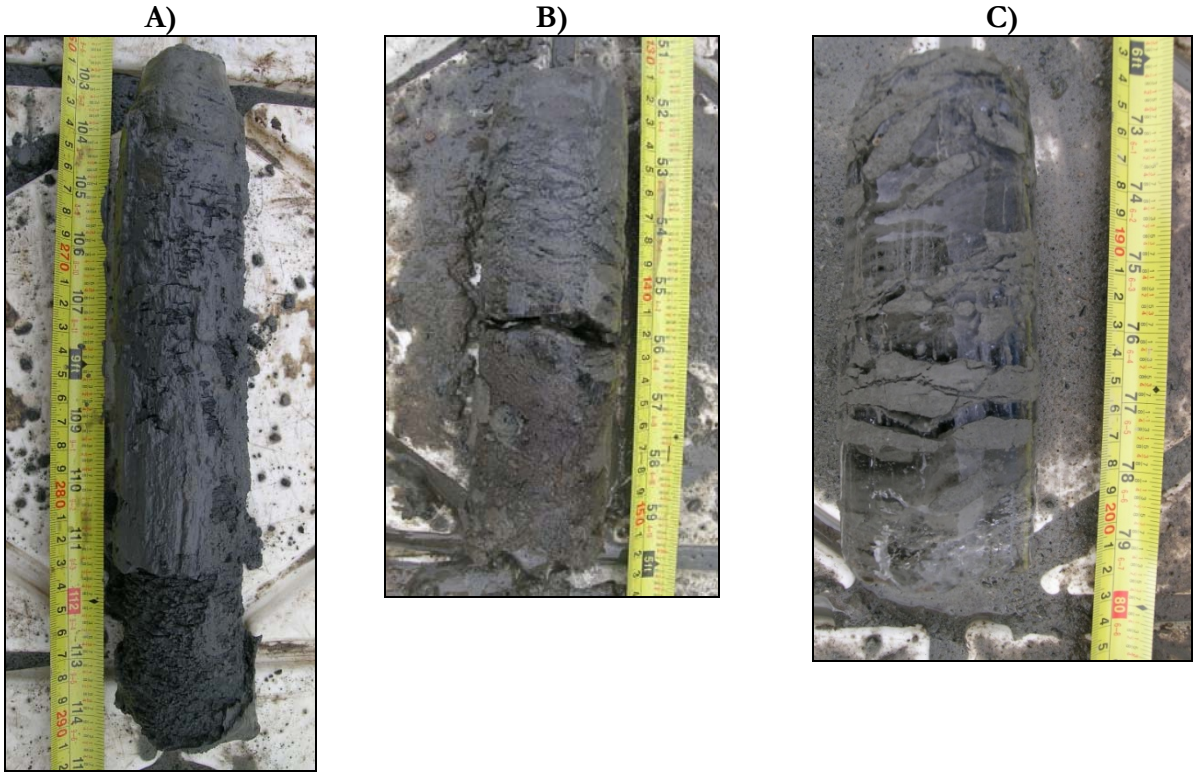

Figure 22: Permafrost core samples taken in A) the marine sediments (SDH-10), B) colluvial blanket (SDH-11), and C) ice-rich colluvium (SDH-06). See Figure 2 for site locations.

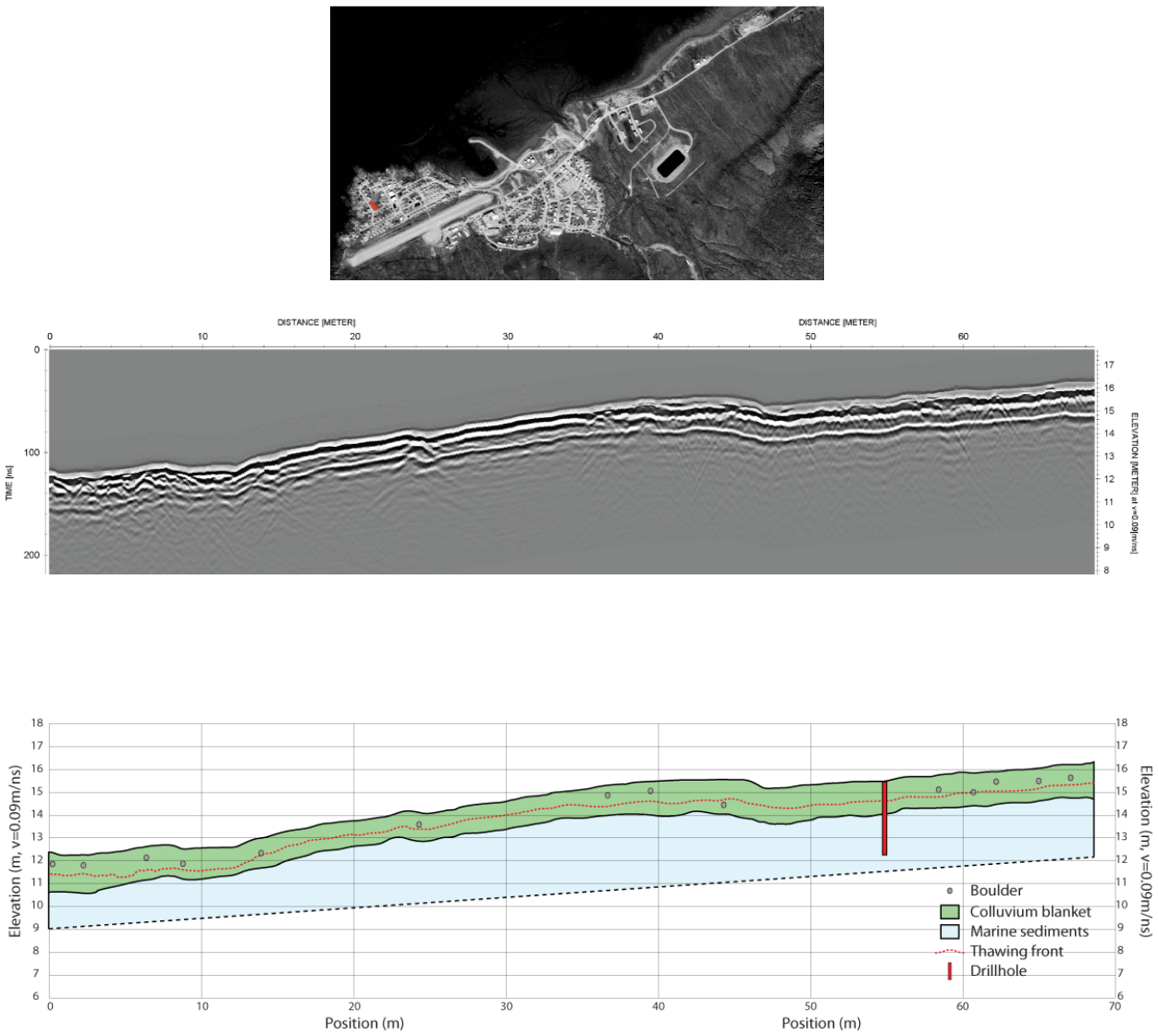

Figure 23 : GPR profile and interpreted cross-section along the SDH-10 section in the marine sediments show a 2 m thick sandy colluvium layer over marine silts into which the electromagnetic signal is absorbed (lost).

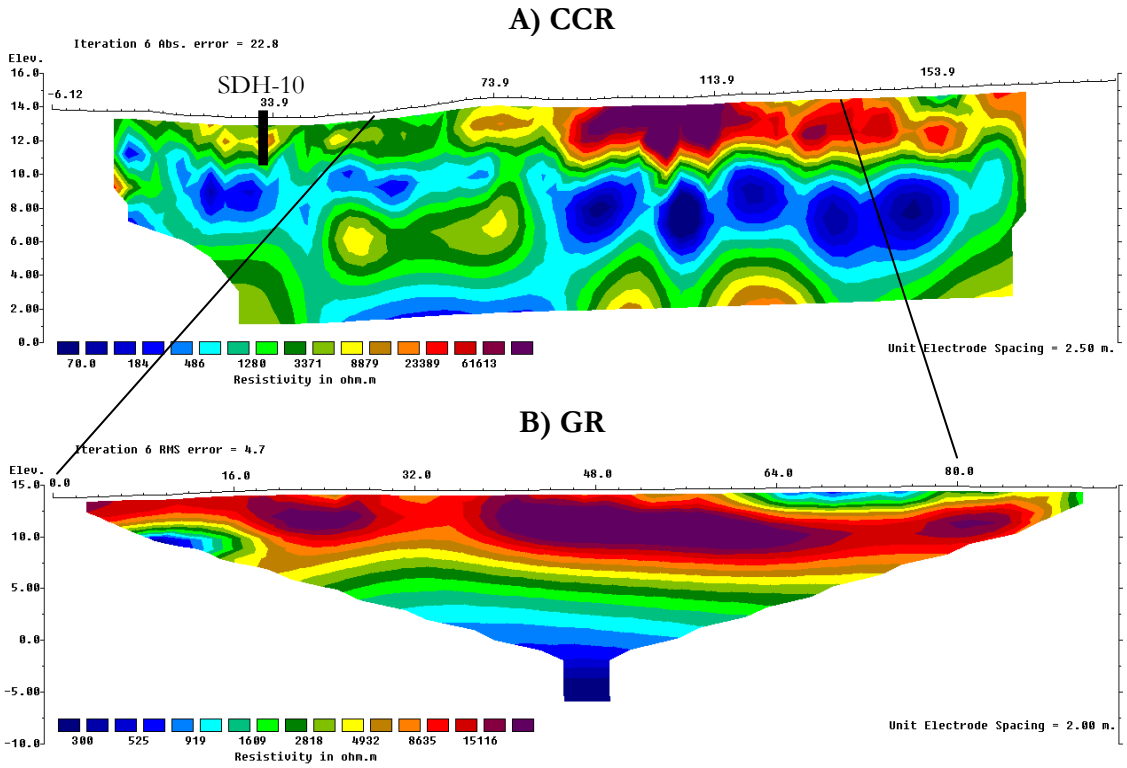

Figure 24 : A) CCR and B) GR resistivity models along the SDH-10 section. The 0 m position on the GR section corresponds to approximately 51 m on the CCR section.

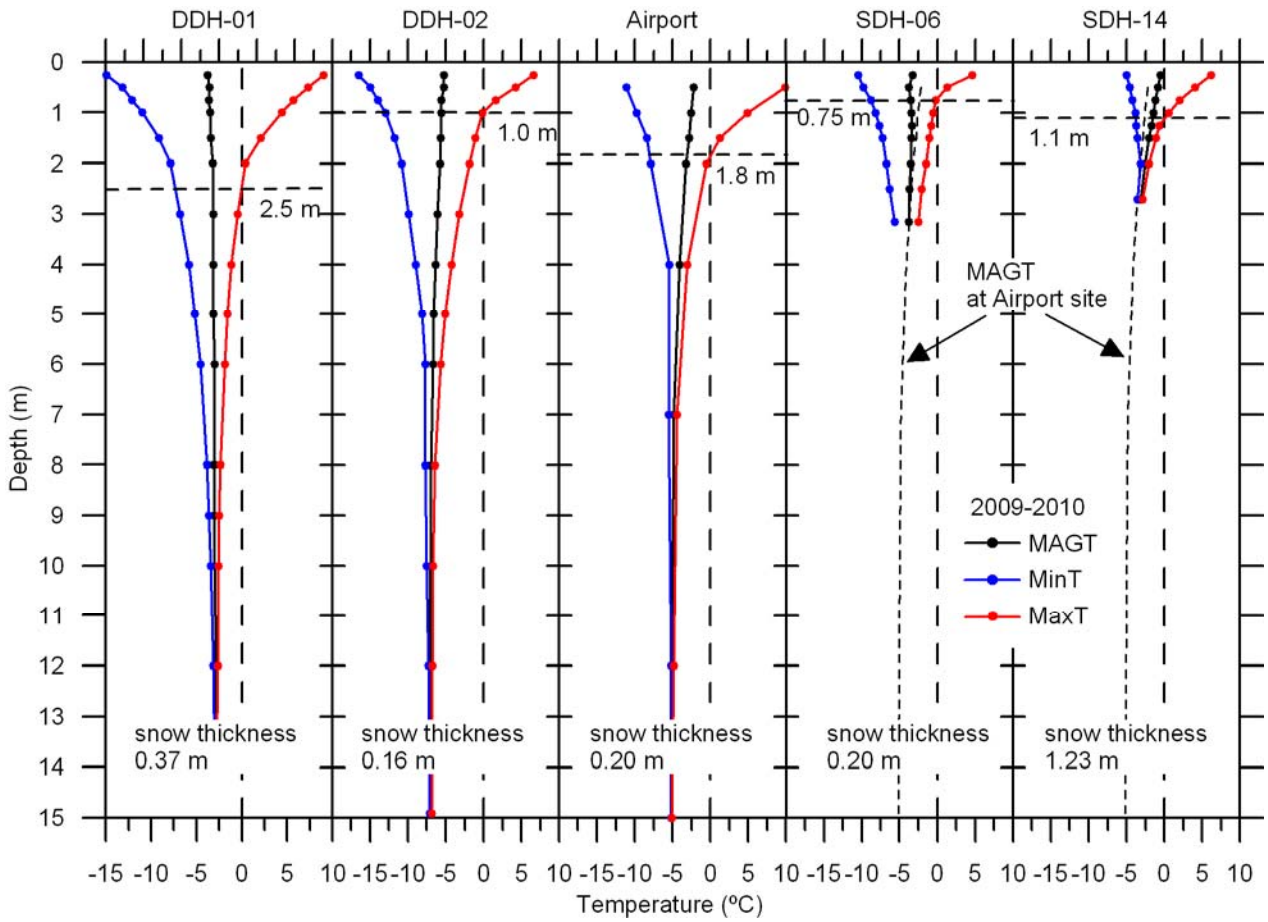

Figure 25: Minimum, maximum and mean annual ground temperatures (MinT, MaxT, MAGT) from August 2009 to July 2010. The maximum active layer is shown for each site, as is snow thickness (March 2010). See Figure 2 for site locations.

Figure 26: Snow bank along the Duval River. Icings, flowing water from the ground that freezes on contact with air, were observed.

APPENDIX A: GROUND PENETRATING RADAR SURVEYS

Ground penetrating radar survey lines

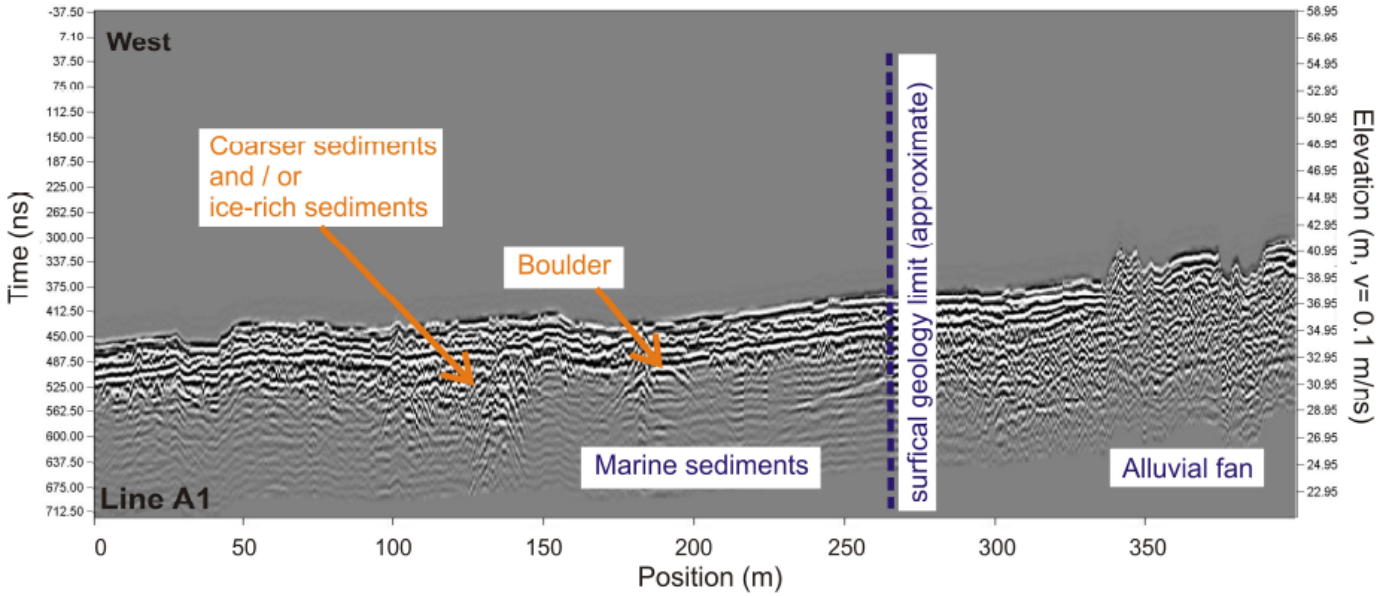
West
Coarser sediments
and / or
ice-rich sediments
Boulder
surfical geology limit (approximate)
Marine sediments
Alluvial fan
Line A1
Time (ns)
Position (m)
Elevation (m, v= 0.1 m/ns)

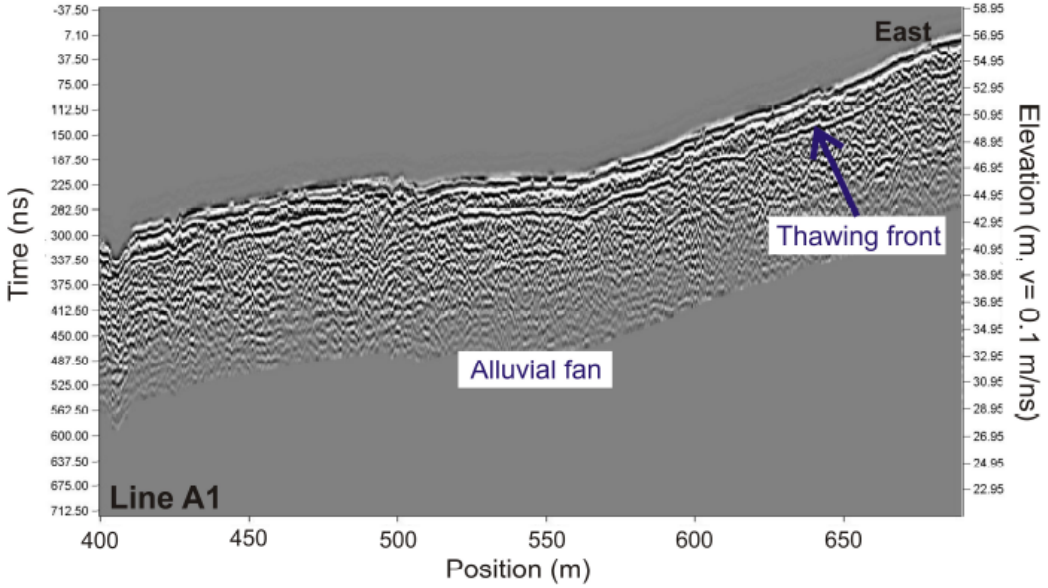
East
Thawing front
Alluvial fan
Line A1
Time (ns)
Position (m)
Elevation (m, v= 0.1 m/ns)

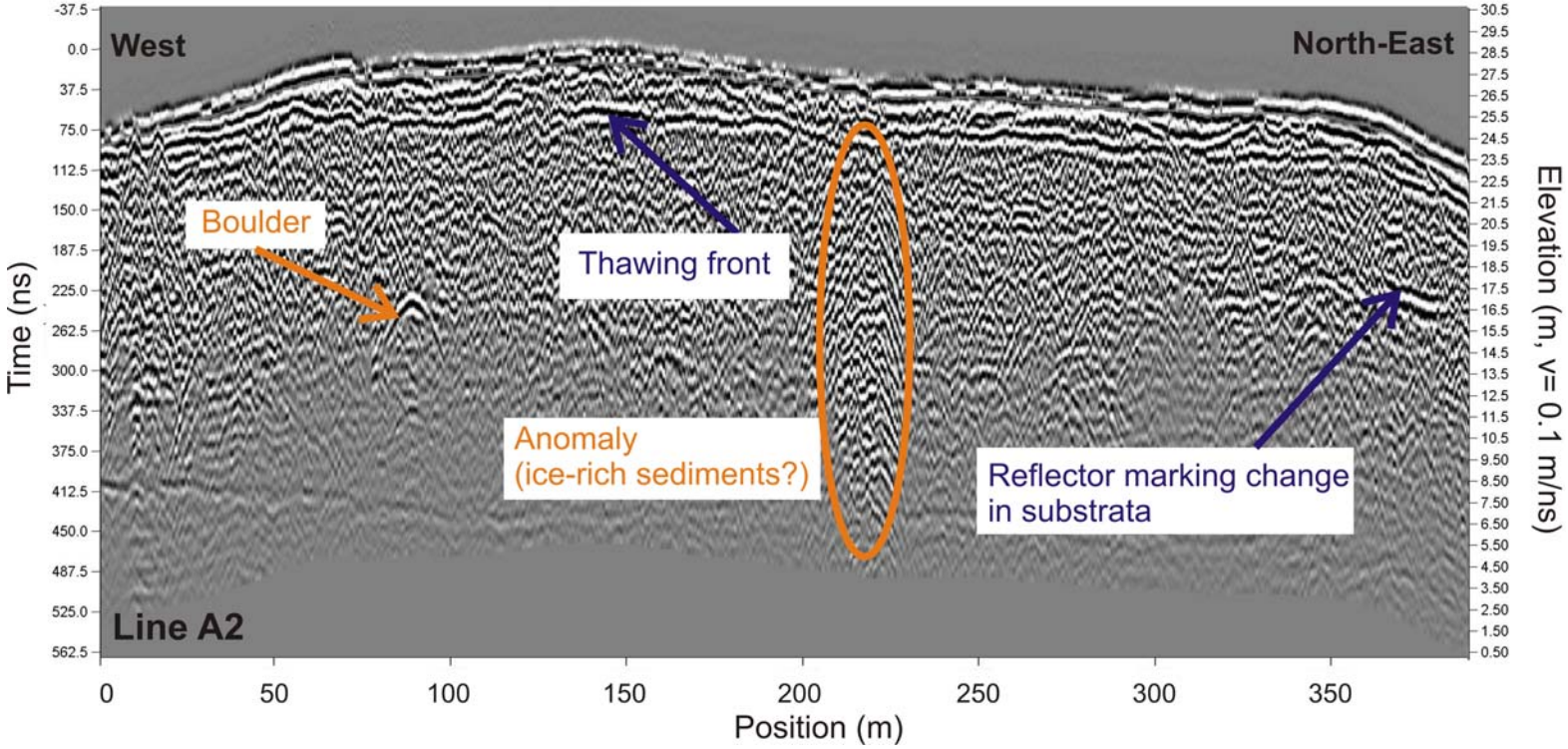
West
North-East
Boulder
Thawing front
Anomaly
(ice-rich sediments?)
Reflector marking change
in substrata
Line A2
Time (ns)
Position (m)
Elevation (m, v= 0.1 m/ns)
-37.5
0.0
37.5
75.0
112.5
150.0
187.5
225.0
262.5
300.0
337.5
375.0
412.5
450.0
487.5
525.0
562.5
0
50
100
150
200
250
300
350
30.5
29.5
28.5
27.5
26.5
25.5
24.5
23.5
22.5
21.5
20.5
19.5
18.5
17.5
16.5
15.5
14.5
13.5
12.5
11.5
10.5
9.50
8.50
7.50
6.50
5.50
4.50
3.50
2.50
1.50
0.50

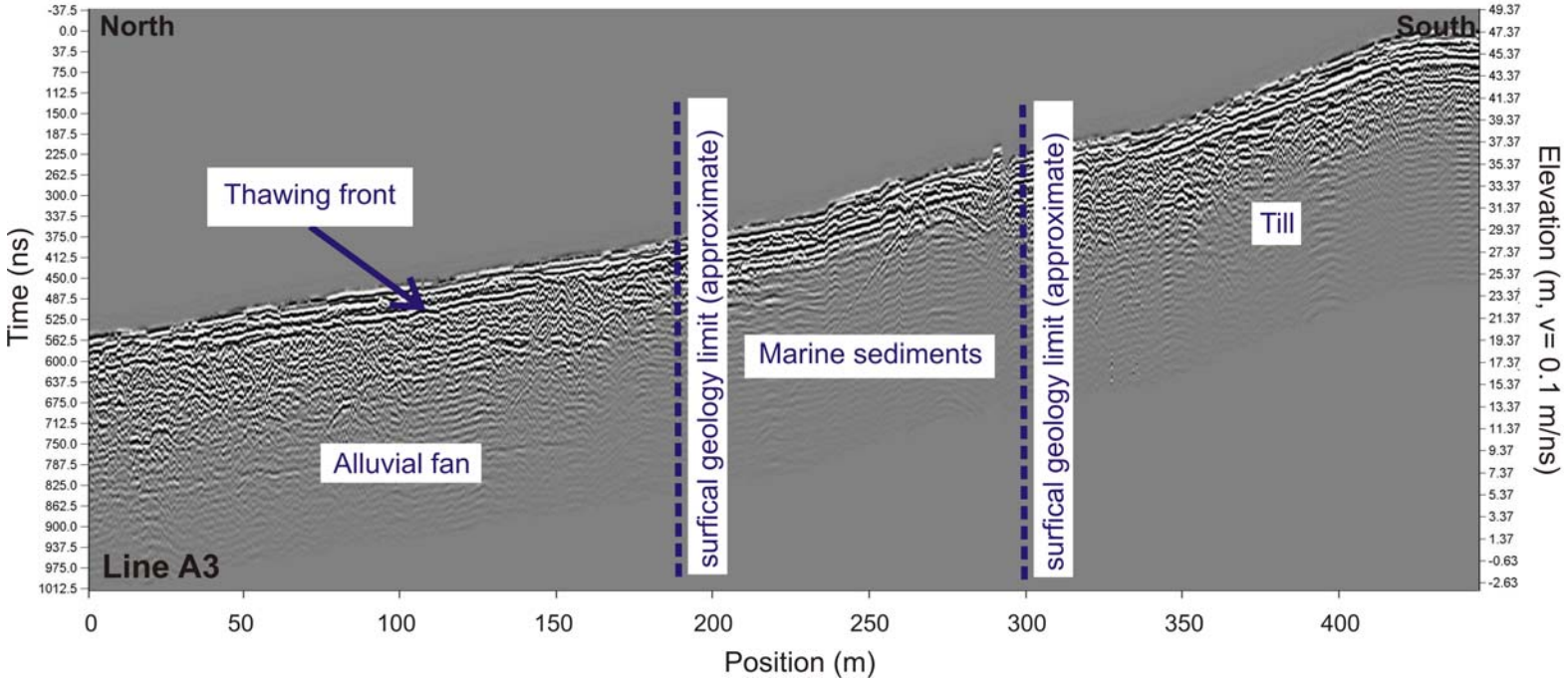
North
South
Thawing front
surfical geology limit (approximate)
surfical geology limit (approximate)
Marine sediments
Till
Alluvial fan
Line A3
Time (ns)
Elevation (m, v= 0.1 m/ns)
Position (m)
0
50
100
150
200
250
300
350
400

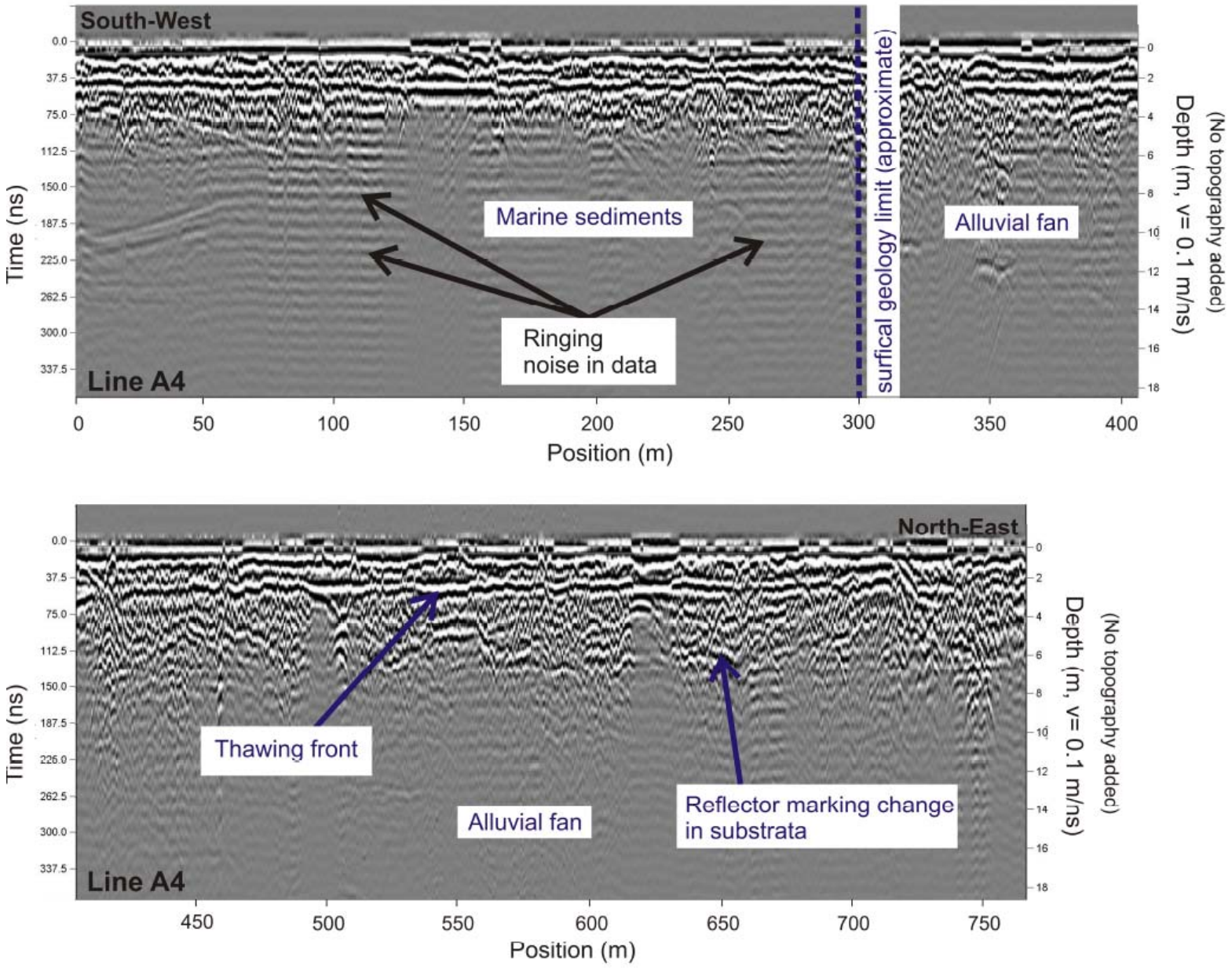
South-West
Marine sediments
Ringing
noise in data
surfical geology limit (approximate)
Alluvial fan
Line A4
Time (ns)
Position (m)
Depth (m, v= 0.1 m/ns)
(No topography added)
North-East
Thawing front
Alluvial fan
Reflector marking change
in substrata
Line A4
Time (ns)
Position (m)
Depth (m, v= 0.1 m/ns)
(No topography added)

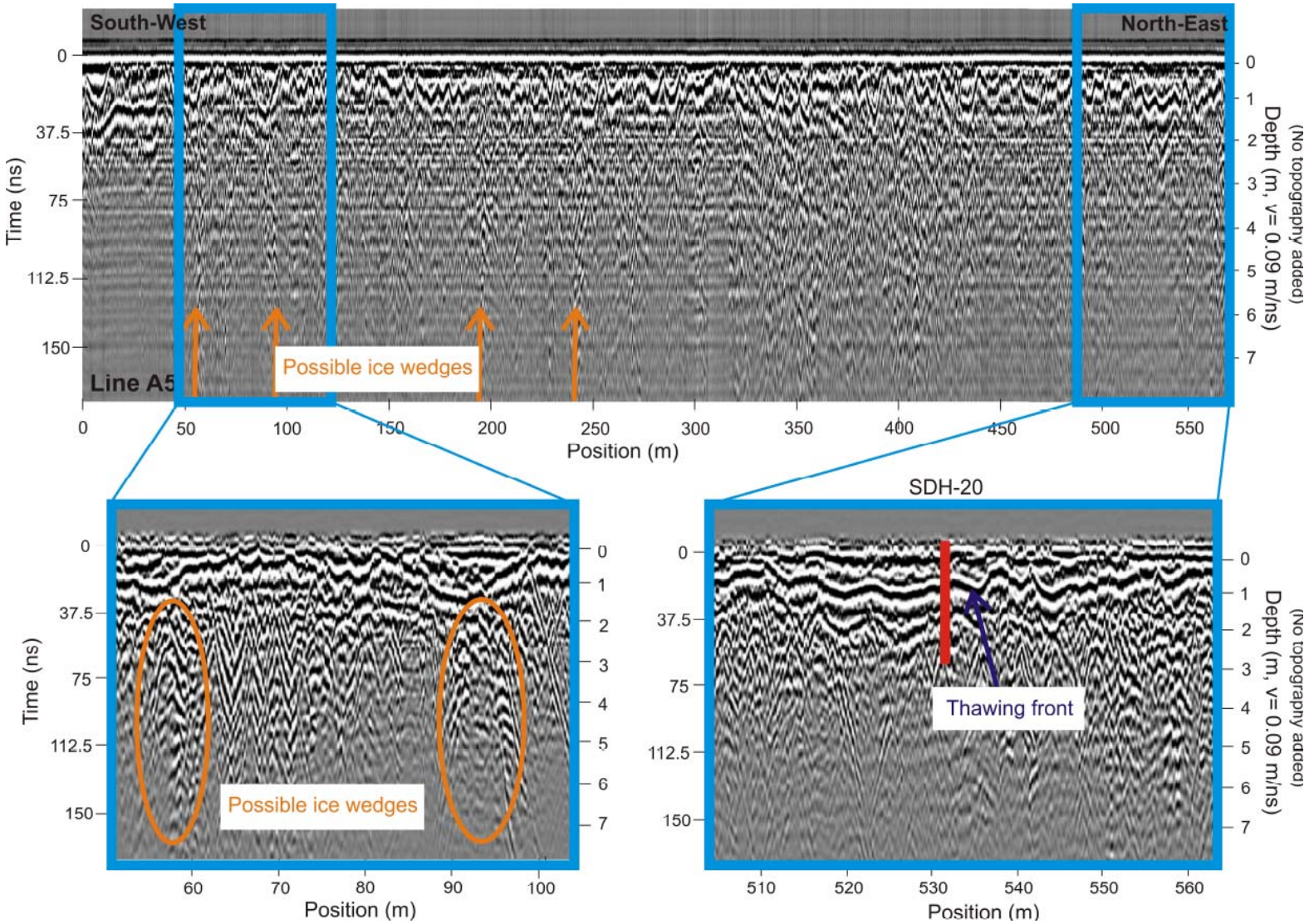
South-West
North-East
Line A5
Possible ice wedges
Time (ns)
Depth (m, v= 0.09 m/ns)
(No topography added)
Position (m)
SDH-20
Possible ice wedges
Thawing front

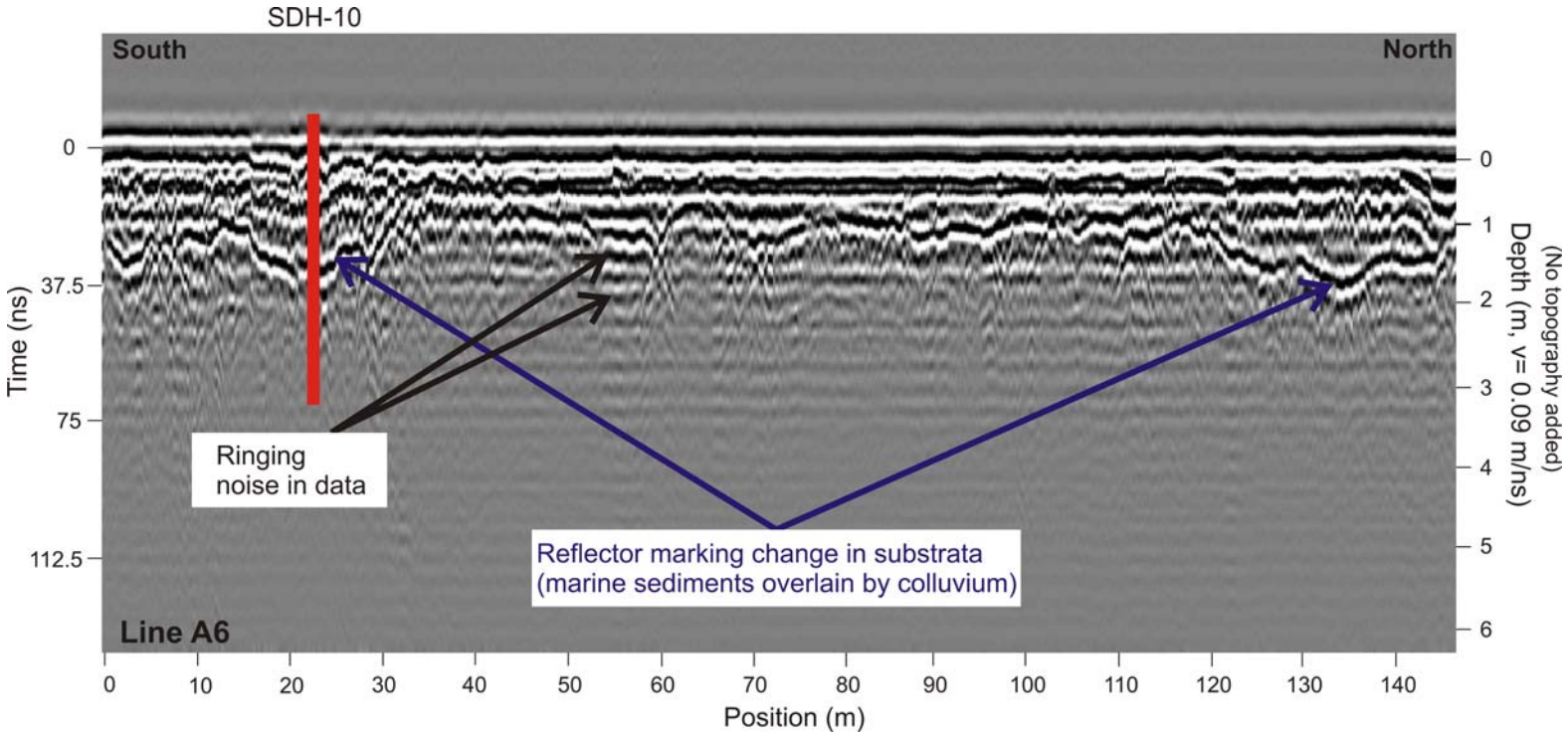
SDH-10
South
North
0
37.5
75
112.5
Time (ns)
Ringing
noise in data
Reflector marking change in substrata
(marine sediments overlain by colluvium)
Line A6
0
10
20
30
40
50
60
70
80
90
100
110
120
130
140
Position (m)
0
1
2
3
4
5
6
Depth (m, v= 0.09 m/ns)
(No topography added)

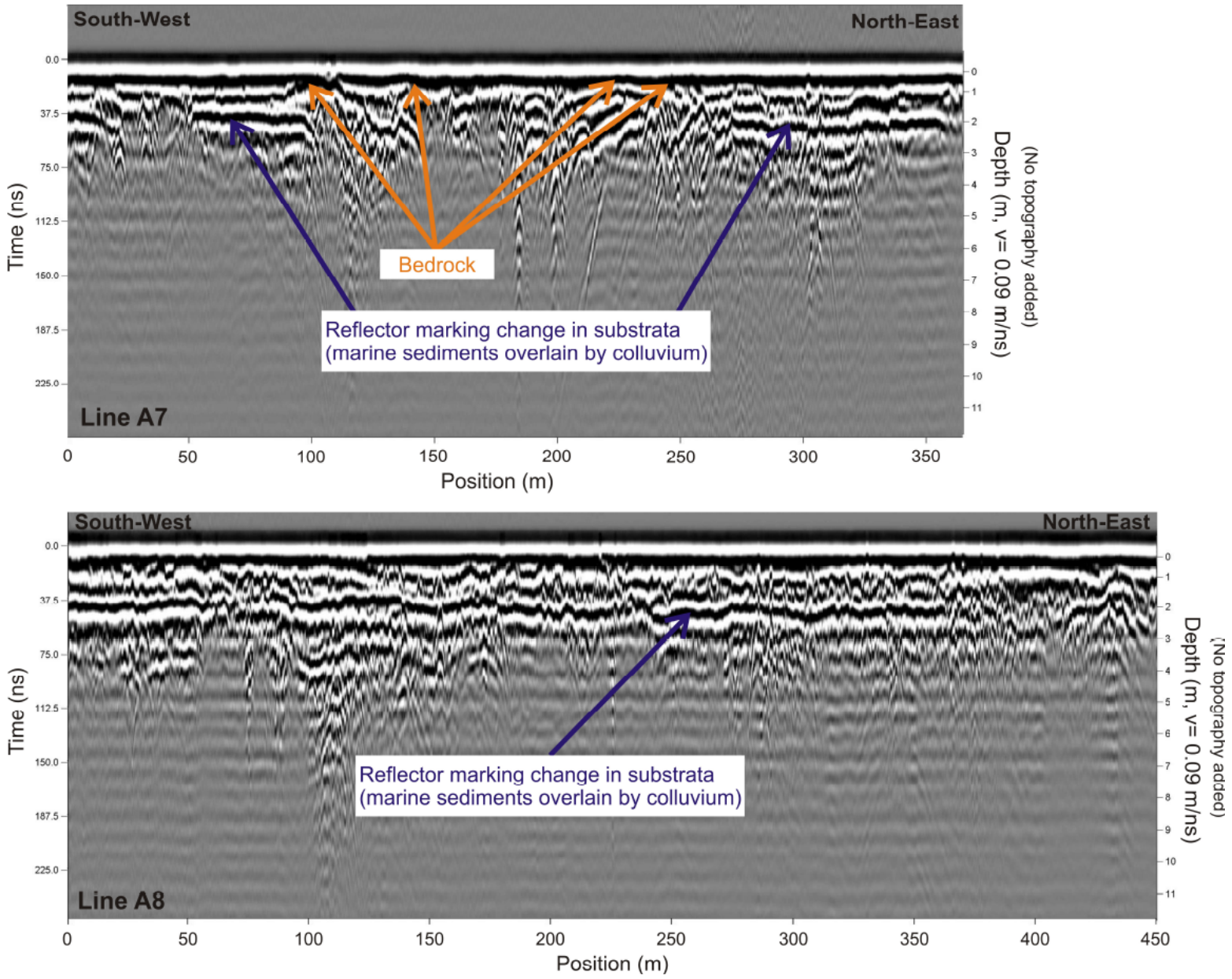
South-West
North-East
Bedrock
Reflector marking change in substrata
(marine sediments overlain by colluvium)
Line A7
Time (ns)
Depth (m, v= 0.09 m/ns)
(No topography added)
Position (m)
South-West
North-East
Reflector marking change in substrata
(marine sediments overlain by colluvium)
Line A8
Time (ns)
Depth (m, v= 0.09 m/ns)
(No topography added)
Position (m)

APPENDIX B : RADIOCARBON DATING

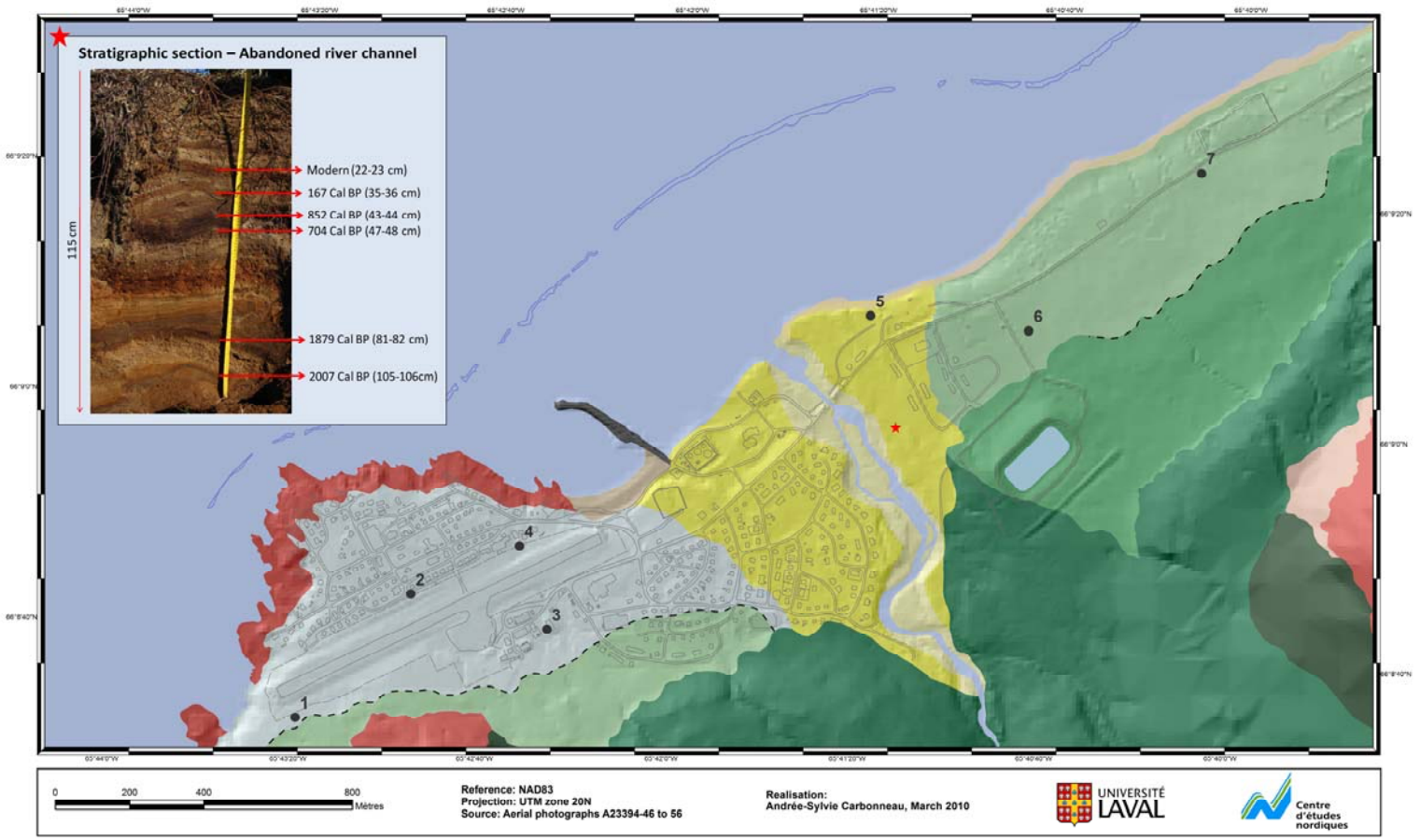

Figure B1

Location of drill holes where buried organic layers and shells where found.

Location on the map	Radiocarbon lab. code	Sample name	Depth (cm)	Elevation (m)	Material	^{14}C date (BP)	Standard deviation in age	Cal BP range 2σ	Cal BP median probability
6	UCIAMS-87499	Pang SDH-02	21,5-22	25	Peat	205	20	0-299	170
7	UCIAMS-87505	Pang SDH-13	43,5-44,5	18	Peat	365	15	325-496	445
6	UCIAMS-87500	Pang SDH-02	37-38	25	Peat	680	15	568-672	660
6	UCIAMS-87501	Pang SDH-02	41-44	25	Peat	755	20	669-723	685
7	UCIAMS-87510	Pang SDH-13	21,5-22,5	18	Peat	990	15	803-951	924
1	UCIAMS-87503	Pang SDH-09	67-72,5	23	Peat	1015	20	917-963	937
7	UCIAMS-87513	Pang SDH-13	46-48,5	18	Peat	1215	15	1069-1223	1137
1	UCIAMS-87509	Pang SDH-09	79,5-83	23	Peat	1695	15	1543-1690	1592
1	UCIAMS-87504	Pang SDH-09	65-66	23	Organic sediment	1890	15	1745-1884	1847
4	UCIAMS-87507	Pang SDH-11	56-58	17	Buried soil	1910	15	1823-1888	1856
4	UCIAMS-87517	Pang SDH-11	54-56	17	Buried soil	1935	15	1828-1925	1884
1	UCIAMS-87508	Pang SDH-09	106-107	22	Peat	1990	20	1893-1990	1939
1	UCIAMS-87516	Pang SDH-09	43-45	23	Organic sediment	3060	15	3219-3345	3295
2	UCIAMS-87514	Pang SDH-08	58-65	22	Buried soil	3360	20	3511-3686	3605
7	UCIAMS-87849	Pang SDH-13	54-56	18	Organic sediment	3520	15	3721-3859	3781
4	UCIAMS-87506	Pang SDH-11	156-157	16	Buried soil	3945	20	4296-4511	4416
2	UCIAMS-87515	Pang SDH-08	77-83	21	Buried soil	4965	20	5624-5740	5690
3	UCIAMS-87502	Pang SDH-06	77-79	25	Buried soil	6190	20	7007-7166	7080
5	UCIAMS-85914	Pang S5	10	9	Shells	8185	25	8210-8594	8517
2	UCIAMS-85913	Pang SDH-08	237-247	20	Shells	9015	25	9378-9823	9553

Table B1 (see Figure B1 for site locations)